A Stochastic Geometry Approach to Coexistence in Heterogeneous Wireless Networks

A Stochastic Geometry Approach to Coexistence in Heterogeneous Wireless Networks

Pedro C. Pinto, *Student Member, IEEE,* Andrea Giorgetti, *Member, IEEE,* Moe Z. Win, *Fellow, IEEE,* and Marco Chiani, *Senior Member, IEEE*

***Abstract*—With the increasing proliferation of different communication devices sharing the same spectrum, it is critical to understand the impact of interference in heterogeneous wireless networks. In this paper, we put forth a mathematical model for coexistence in networks composed of both narrowband (NB) and ultrawideband (UWB) wireless nodes, based on fundamental tools from stochastic geometry. Our model considers that the interferers are spatially scattered according to a Poisson field, and are operating asynchronously in a wireless environment. We first determine the statistical distribution of the aggregate interference for both cases of NB and UWB emitters. We then provide error probability expressions for two dual configurations: 1) a NB victim link subject to the aggregate UWB interference, and 2) a UWB victim link subject to the aggregate NB interference. The results show that while the impact of a *single* interferer on a link is often negligible due to restrictions on the transmitted power, the *aggregate* effect of multiple interferers may cause significant degradation. Therefore, aggregate interference must be considered to ensure coexistence in heterogeneous networks. The proposed analytical framework shows good agreement with physical-level simulations of the system.**

***Index Terms*—Stochastic geometry, ultrawideband systems, narrowband systems, coexistence, aggregate interference, error probability.**

I. Introduction

THERE has been an emerging interest in transmission systems with large bandwidth for both commercial and military applications. For example, ultrawideband (UWB) systems communicate with direct-sequence (DS) or time-hopping (TH) spread-spectrum (SS) signals using a train of extremely short pulses, thereby spreading the energy of the signal very thinly over several GHz [1]–[10].

However, the successful deployment of such technologies requires that UWB and narrowband (NB) systems do not interfere with one another. In particular, UWB devices must not cause harmful interference to existing NB systems (e.g., GPS, GSM, and IEEE 802.11), and at the same time must be robust to NB interference.

The issue of coexistence in heterogeneous networks has received considerable attention lately. Concerning UWB interference on NB systems, the bit error probability (BEP) is analyzed in [11] for the case of a single UWB pulse interfering with a binary phase shift keying (BPSK) NB system, in an additive white Gaussian noise (AWGN) channel. In [12], a semi-analytical BEP expression is derived for the case of one SS signal interfering with a NB-BPSK system, also in an AWGN channel. Using a shot noise perspective, [13] analyzes the combined energy of multiple UWB signals at the output of a square-law receiver, without taking into account the error performance. Concerning the NB interference on UWB systems, the analysis has been largely focused on AWGN channels. The BEP of DS-SS systems in an AWGN channel is derived in [14] for one tone interferer, and an upper bound is given in [15] and [16] for multiple tone interferers. A comparison of several multiple-access techniques is made in [17]. The performance of UWB TH-SS systems in the presence of one Gaussian interferer is analyzed in [18] by ignoring AWGN. The effects of GSM and UMTS/WCDMA systems on UWB DS and TH systems in AWGN channel is investigated in [19]–[21]. Closed-form BEP expressions for a UWB system with Rake reception in frequency-selective multipath fading channels subject to a single NB interferer (NBI) is derived in [22]. A comprehensive study of UWB receiver design in the presence of multiple-access UWB interference is provided in [23]. An overview of coexistence issues between UWB and NB wireless communication systems is given in [24]. A mathematical model for the characterization of network interference is developed in [25], and several applications are analyzed. Concerning the stochastic modeling of node positions, the Poisson point process has been successfully used in [26], [27] to analyze interference in wireless networks, although the focus is on simple NB channel models, which are not suitable to study coexistence with UWB systems.

In this paper, we are interested in the coexistence between heterogeneous systems in large-scale wireless networks. The main contributions of this paper are as follows:

- *Framework for coexistence in stochastic networks:* Using notions from stochastic geometry, we introduce a mathematical model for coexistence in heterogeneous wireless networks. Our framework considers UWB and NB interferers which are spatially scattered according to a Poisson field [28]–[31]. In addition, we consider realistic

Manuscript received 30 August 2008; revised 31 January 2009. This research was supported, in part, by the Portuguese Science and Technology Foundation under grant SFRH-BD-17388-2004; the MIT Institute for Soldier Nanotechnologies; the Office of Naval Research under Presidential Early Career Award for Scientists and Engineers (PECASE) N00014-09-1-0435; the National Science Foundation under grant ECS-0636519; the Charles Stark Draper Laboratory Reduced Complexity UWB Communication Techniques Program; the European Commission under the FP7 ICT integrated project Co-Existing Short Range Radio by Advanced Ultra-WideBand Radio Technology (EUWB) grant 215669; and the Institute of Advanced Study Natural Science & Technology Fellowship. This work was presented, in part, at the IEEE International Symposium on Spread Spectrum Techniques and Applications, Manaus, Brazil, Aug. 2006, and at the IEEE International Conference on Ultra Wideband, Waltham, MA, Sep. 2006.

Pedro C. Pinto and Moe Z. Win are with LIDS, Massachusetts Institute of Technology, Cambridge, MA 02139, USA (e-mail: {ppinto, moewin}@mit.edu).

Andrea Giorgetti and Marco Chiani are with DEIS, WiLAB, University of Bologna, 47023 Cesena ITALY (e-mail: {andrea.giorgetti, marco.chiani}@unibo.it).

Digital Object Identifier 10.1109/JSAC.2009.090922.

NB and UWB channel models which account for path loss, shadowing, and multipath fading.

- *NB communication in the presence of UWB interferers:* We provide a probabilistic characterization of the aggregate UWB interference generated by all nodes in the network. We then provide expressions for average and outage error probability of a NB victim link in the presence of such aggregate UWB interference.
- *UWB communication in the presence of NB interferers:* We also consider the dual scenario, by first providing a probabilistic characterization of the aggregate NB interference generated by all nodes in the network. We then provide expressions for both average and outage error probability of a UWB victim link in the presence of such aggregate NB interference.

The paper is organized as follows. Section II presents the system model. Section III characterizes NB communication in the presence of UWB interferers. Section IV analyzes UWB communication in the presence of NB interferers. Section V presents numerical results for some practical coexistence scenarios, illustrating the dependence of the error probability on network parameters such as the signal-to-noise ratio (SNR), interference-to-noise ratio (INR), path loss exponent, and spatial density of the interferers. Section VI concludes the paper and summarizes important findings.

II. System Model

We start by describing our system model. The notation and symbols used throughout the paper are summarized in Table III in the end of this paper.

A. Spatial Distribution of the Nodes

The spatial distribution of the interferers is modeled according to a homogeneous Poisson point process $\Pi \subset \mathbb{R}^2$ with spatial density λ, in nodes per unit area [32]. Typically, the node positions are unknown to the network designer a priori, so they may as well be treated as completely random according to a spatial Poisson process.[1] We define the *interfering nodes* to be the set of terminals which are transmitting within the frequency band of interest, during the time interval of interest (e.g., one symbol period), and hence are effectively contributing to the total interference. Thus, irrespective of the network topology (e.g., point-to-point mode or broadcast mode) or the session lifetime of each interferer, the proposed model depends only on the effective density λ of interfering nodes.[2]

The proposed spatial model is depicted in Fig. 1. Here, we consider a victim link composed of two nodes: one receiver node, located at the origin of the two-dimensional plane, and one transmitter node (node $i = 0$), deterministically located at a distance r_0 from the origin. All the other nodes ($i = 1, 2, \ldots, \infty$) are interfering nodes, whose random distances to the origin are denoted by $\{R_i\}_{i=1}^{\infty}$, where $R_1 \leq R_2 \leq \ldots$. Our goal is then to determine: 1) the effect of UWB interfering nodes on a NB victim link, as shown in Fig 1(a); and 2) the effect of NB interfering nodes on a UWB victim link, as shown in Fig 1(b).

[1]The spatial Poisson process is a natural choice in such situation because, given that a node is inside a region $\mathcal{R}$, the p.d.f. of its position is conditionally uniform over $\mathcal{R}$.

[2]For example, if the interfering nodes are idle for a fraction of the time, then the splitting property of Poisson processes [33] can be used to obtain the *effective* density of nodes that contribute to the interference.

B. Transmission Characteristics of the Nodes

We consider the case where the UWB (or NB) interferers operate asynchronously and independently, using the same power P_{U} (or P_{N}). This is a plausible constraint in the absence of power control and is applicable in many decentralized ad-hoc networks, WLANs, and WPANs. The signal $s_i^{\mathrm{U}}(t)$ transmitted by the ith UWB interferer can be described as

$$s_i^{\mathrm{U}}(t) = \sqrt{2E_{\mathrm{U}}} \sum_{n=-\infty}^{\infty} a_{i,n}^{\mathrm{U}} w_i(t - nT_{\mathrm{U}} - D_i) \times \cos\left(2\pi f_{\mathrm{U}}(t - D_i) + \theta_{i,n}^{\mathrm{U}}\right), \quad (1)$$

where E_{U} is the average transmitted symbol energy; $P_{\mathrm{U}} = E_{\mathrm{U}}/T_{\mathrm{U}}$ is the average transmitted power; $w_i(t)$ is the unit-energy symbol waveform; $a_{i,n}^{\mathrm{U}} e^{j\theta_{i,n}^{\mathrm{U}}}$ is the nth transmitted symbol of the ith UWB interferer, belonging to a constellation $\mathcal{C}^{\mathrm{U}} = \{\mathbf{s}_1^{\mathrm{U}}, \ldots, \mathbf{s}_M^{\mathrm{U}}\}$,[3] and satisfying $\mathbb{E}\{(a_{i,n}^{\mathrm{U}})^2\} = 1$; T_{U} is the symbol period; f_{U} is the carrier frequency of the UWB signal; and $D_i \sim \mathcal{U}(0, T_{\mathrm{U}})$[4] is a random delay modeling the asynchronism between nodes.

The signal $s_i^{\mathrm{N}}(t)$ transmitted by the ith NB interferer can be written as

$$s_i^{\mathrm{N}}(t) = \sqrt{2E_{\mathrm{N}}} \sum_{n=-\infty}^{\infty} a_{i,n}^{\mathrm{N}} g(t - nT_{\mathrm{N}} - D_i) \times \cos\left(2\pi f_{\mathrm{N}}(t - D_i) + \theta_{i,n}^{\mathrm{N}}\right), \quad (2)$$

where E_{N} is the average transmitted symbol energy; $P_{\mathrm{N}} = E_{\mathrm{N}}/T_{\mathrm{N}}$ is the average transmitted power; $g(t)$ is a unit-energy pulse-shaping waveform satisfying the Nyquist criterion; $a_{i,n}^{\mathrm{N}} e^{j\theta_{i,n}^{\mathrm{N}}}$ is the nth transmitted symbol of the ith NB interferer, belonging to a constellation $\mathcal{C}^{\mathrm{N}} = \{\mathbf{s}_1^{\mathrm{N}}, \ldots, \mathbf{s}_M^{\mathrm{N}}\}$, and satisfying $\mathbb{E}\{(a_{i,n}^{\mathrm{N}})^2\} = 1$; T_{N} is the symbol period; and f_{N} is the carrier frequency of the NB signal. In (1) and (2), we consider that the random variables (r.v.'s) $a_{i,n}$, $\theta_{i,n}$, and D_i are i.i.d in i (since interferers operate independently) and in n.

Example of UWB Systems: For impulse radio (IR) SS systems with DS and TH, the unit-energy symbol waveform $w(t)$ in (1) is given by

$$w(t) = \sum_{k=0}^{N_{\mathrm{s}}-1} c_k^{\mathrm{DS}} p(t - kT_{\mathrm{f}} - c_k^{\mathrm{TH}} T_{\mathrm{c}}), \quad (3)$$

where N_{s} is the number of pulses used to transmit a single information symbol belonging to a two-dimensional constellation, and $p(t)$ is the transmitted monocycle shape, with energy $1/N_{\mathrm{s}}$. The pulse repetition time (frame length) T_{f} and the symbol duration T_{U} are related by $T_{\mathrm{U}} = N_{\mathrm{s}} T_{\mathrm{f}}$. Finally, $\{c_k^{\mathrm{DS}}\}_{k=0}^{N_{\mathrm{s}}-1}$ is the DS sequence, $\{c_k^{\mathrm{TH}}\}_{k=0}^{N_{\mathrm{s}}-1}$ is the TH sequence, and T_{c} is the TH chip width. The symbol waveform given in

[3]We use boldface letters to denote complex quantities.

[4]We use $\mathcal{U}(a, b)$ to denote a real uniform distribution in the interval $[a, b]$.

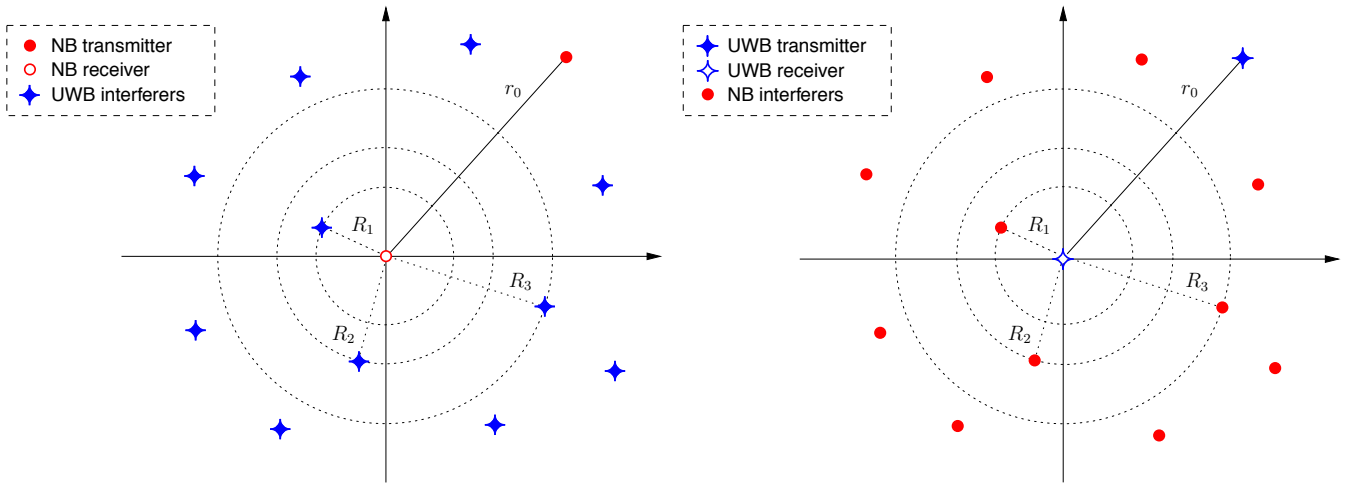

(a) NB victim link, UWB interferers.

(b) UWB victim link, NB interferers.

Fig. 1. Poisson field model for the spatial distribution of nodes. Without loss of generality, we assume the origin of the coordinate system coincides with the victim receiver.

(3) is valid for a general transmission scheme that combines DS and TH, and results in a pure DS when $c_k^{\mathrm{TH}} = 0$, $\forall k$, and a pure TH when $c_k^{\mathrm{DS}} = 1$, $\forall k$. The Fourier transform of $w(t)$ given in (3) is

$$\mathbf{W}(f) = P(f) \sum_{k=0}^{N_s-1} c_k^{\mathrm{DS}} e^{-j2\pi f(kT_f + c_k^{\mathrm{TH}} T_c)} \tag{4}$$

where $P(f) \triangleq \mathcal{F}\{p(t)\}$.[5]

C. Propagation Characteristics of the Medium

To account for the propagation characteristics affecting both the NB and UWB nodes, we consider that the median of the signal amplitude decays with the distance r according to k/r^{ν}, for some given constant k and $\nu > 1$. Although the amplitude loss exponent ν typically ranges from 0.8 (e.g., hallways inside buildings) to 4 (e.g., dense urban environments) [34], [35], we consider only the case of $\nu > 1$. The use of such a decay law also ensures that interferers located far away have negligible contribution to the total interference observed at the victim receiver, thus making the infinite-plane model reasonable. For generality, we assume different path loss parameters for the NB signal (k_{N}, ν_{N}) and the UWB signals (k_{U}, ν_{U}).

To capture the shadowing affecting both NB and UWB nodes, we use a lognormal model where the received signal strength S is given by $S = \mu e^{\sigma G}$, where $G \sim \mathcal{N}(0,1)$ and independent of everything else,[6] $\mu = k/r^{\nu}$ is the median of S, and σ is the shadowing coefficient.[7] The shadowing is responsible for random fluctuations in the signal level around the median path gain k/r^{ν}. For generality, we assume different shadowing parameters for the NB signal (σ_{N}) and the UWB signals (σ_{U}).

[5]We use $\mathcal{F}\{\cdot\}$ to denote the Fourier transform operator.

[6]We use $\mathcal{N}(0,\sigma^2)$ to denote a real, zero-mean, Gaussian distribution with variance σ^2.

[7]This model for combined path loss and log-normal shadowing can be expressed in logarithmic form [35], [36], such that the channel loss in dB is given by $L_{\mathrm{dB}} = k_0 + k_1 \log_{10} r + \sigma_{\mathrm{dB}} G$, where $G \sim \mathcal{N}(0,1)$. The environment-dependent parameters $(k_0, k_1, \sigma_{\mathrm{dB}})$ can be related to (k, ν, σ) as follows: $k_0 = -20\log_{10} k$, $k_1 = 20\nu$, and $\sigma_{\mathrm{dB}} = \frac{20}{\ln 10}\sigma$. The parameter σ_{dB} is the standard deviation of the channel loss in dB (or, equivalently, of the received SNR in dB).

To account for the fading affecting the UWB nodes, we consider a frequency-selective multipath channel with impulse response

$$h_i(t) = \sum_{q=1}^{L} h_{i,q}\delta(t - t_{i,q}), \tag{5}$$

where $\{h_{i,q}\}_{q=1}^{L}$ and $\{t_{i,q}\}_{q=1}^{L}$ are, respectively, the amplitudes and delays (with arbitrary statistics) describing the L paths which affect the ith UWB interferer; and $\delta(t)$ denotes the Dirac-delta function. In addition, we normalize the power dispersion profile (PDP) of the channel such that $\sum_{q=1}^{L} \mathbb{E}\{h_{i,q}^2\} = 1$. On the other hand, we model the fading affecting the NB nodes using a frequency-flat Rayleigh channel. Specifically, the channel introduces in the received NB signal a Rayleigh-distributed amplitude factor α_i (normalized so that $\mathbb{E}\{\alpha_i^2\} = 1$), as well as a uniform phase ϕ_i.

Considering the previously described propagation effects (path loss, shadowing, and fading), the overall channel impulse response (CIR) between the ith UWB interferer and the NB victim receiver (Fig. 1(a)) becomes

$$\widetilde{h}_i^{\mathrm{U}}(t) = \frac{k_{\mathrm{U}}}{R_i^{\nu_{\mathrm{U}}}} e^{\sigma_{\mathrm{U}} G_i} h_i(t). \tag{6}$$

On the other hand, the overall CIR between the ith NB interferer and the UWB victim receiver (Fig.1(b)) becomes

$$\widetilde{h}_i^{\mathrm{N}}(t) = \frac{k_{\mathrm{N}}}{R_i^{\nu_{\mathrm{N}}}} \alpha_i e^{\sigma_{\mathrm{N}} G_i} \delta(t - t_i), \tag{7}$$

where $t_i = \phi_i/(2\pi f_{\mathrm{N}})$. In this paper, we assume the shadowing and the fading to be independent for different interferers i, and approximately constant during at least one symbol interval.

D. Mobility of the Interferers

Typically, the time variation of the distances $\{R_i\}_{i=1}^{\infty}$ of the interferers is highly coupled with that of the shadowing $\{G_i\}_{i=1}^{\infty}$ affecting those nodes. This is because the shadowing is itself associated with the movement of the nodes near large blocking objects. Thus, we introduce the notation $\mathcal{P}$ to

$$\mathbf{X}_i = k_{\mathrm{U}}\sqrt{2E_{\mathrm{U}}}\sum_{n=-\infty}^{\infty} a_{i,n}^{\mathrm{U}} \int_{-\infty}^{+\infty} \left\{ \left[w_i(t-\widetilde{D}_{i,n}) \cos\left(2\pi f_{\mathrm{U}}(t-D_i)+\theta_{i,n}^{\mathrm{U}}\right)\right] * h_i(t) \right\} \cdot \boldsymbol{\psi}(t)dt \tag{11}$$

denote *"the distances $\{R_i\}_{i=1}^{\infty}$ and shadowing $\{G_i\}_{i=1}^{\infty}$ of the interferers."* In this paper, we carry out two types of analysis:

1) $\mathcal{P}$-conditioned analysis: We *condition* the interference on a given realization of $\mathcal{P}$, which naturally leads to the derivation of the *outage error probability* of the victim link [37]–[41].
2) $\mathcal{P}$-averaged analysis: We *average* the interference over all possible realizations of $\mathcal{P}$, which naturally leads to the derivation of the *average error probability* of the victim link [42]–[46].

III. NB Communication in the Presence of UWB Interferers

A. Signals and Interference Models

Under the system model described in Section II, the aggregate signal $z(t)$ at the NB receiver can be written as[8]

$$z(t) = d(t) + y(t) + n(t),$$

where $d(t) = \left[\sqrt{2E_{\mathrm{N}}}\, a_0^{\mathrm{N}} g(t)\cos(2\pi f_{\mathrm{N}} t + \theta_0^{\mathrm{N}})\right] * \widetilde{h}_0^{\mathrm{N}}(t)$ is the desired signal from the NB transmitter corresponding to symbol $n = 0$,[9] with $*$ denoting the convolution operator; $y(t) = \sum_{i=1}^{\infty} s_i^{\mathrm{U}}(t) * \widetilde{h}_i^{\mathrm{U}}(t)$ is the aggregate network interference; and $n(t)$ is the AWGN with two-sided power spectral density (PSD) $N_0/2$, and independent of $y(t)$. By performing the indicated convolutions, we can further express the desired signal as

$$d(t) = \frac{k_{\mathrm{N}}\alpha_0 e^{\sigma_{\mathrm{N}} G_0}}{r_0^{\nu_{\mathrm{N}}}} \sqrt{2E_{\mathrm{N}}}\, a_0^{\mathrm{N}} g(t)\cos(2\pi f_{\mathrm{N}} t + \theta_0^{\mathrm{N}}),$$

and the aggregate interference as

$$y(t) = \sqrt{2E_{\mathrm{U}}}\sum_{i=1}^{\infty} \frac{k_{\mathrm{U}} e^{\sigma_{\mathrm{U}} G_i}}{R_i^{\nu_{\mathrm{U}}}} \sum_{n=-\infty}^{\infty} a_{i,n}^{\mathrm{U}} \times \left[w_i(t - nT_{\mathrm{U}} - D_i)\cos\left(2\pi f_{\mathrm{U}}(t-D_i)+\theta_{i,n}^{\mathrm{U}}\right)\right] * h_i(t).$$

The NB receiver demodulates the aggregate signal $z(t)$ using a conventional linear detector. This can be achieved by projecting $z(t)$ onto the orthonormal set

$$\psi_1(t) = \sqrt{2} g(t)\cos(2\pi f_{\mathrm{N}} t),$$
$$\psi_2(t) = -\sqrt{2} g(t)\sin(2\pi f_{\mathrm{N}} t).$$

Defining $\mathbf{Z} = Z_1 + jZ_2 = \int_{-\infty}^{+\infty} z(t)\boldsymbol{\psi}(t)dt$, where $\boldsymbol{\psi}(t) = \psi_1(t) + j\psi_2(t) = \sqrt{2} g(t) e^{-j2\pi f_{\mathrm{N}} t}$, we can write

$$\mathbf{Z} = \frac{k_{\mathrm{N}}\alpha_0 e^{\sigma_{\mathrm{N}} G_0}}{r_0^{\nu_{\mathrm{N}}}} \sqrt{E_{\mathrm{N}}}\, a_0^{\mathrm{N}} e^{j\theta_0^{\mathrm{N}}} + \mathbf{Y} + \mathbf{N} \tag{8}$$

where the distribution of $\mathbf{N}$ is given by[10]

$$\mathbf{N} \sim \mathcal{N}_{\mathrm{c}}(0, N_0). \tag{9}$$

[8]Note that the signals $d(t)$, $y(t)$, and $n(t)$ are all real-valued, since we do not employ the notion of equivalent low-pass representation in this paper.

[9]To derive the error probability of the NB victim link, we only need to analyze a single NB symbol.

[10]We use $\mathcal{N}_{\mathrm{c}}(0,\sigma^2)$ to denote a circularly symmetric (CS) complex Gaussian distribution, where the real and imaginary parts are i.i.d. $\mathcal{N}(0,\sigma^2/2)$.

Furthermore, $\mathbf{Y} = \int_{-\infty}^{+\infty} y(t)\boldsymbol{\psi}(t)dt$ can be expressed as

$$\mathbf{Y} = \sum_{i=1}^{\infty} \frac{e^{\sigma_{\mathrm{U}} G_i}\mathbf{X}_i}{R_i^{\nu_{\mathrm{U}}}}, \tag{10}$$

where $\mathbf{X}_i$ is given in (11) at the top of this page, with $\widetilde{D}_{i,n} \triangleq nT_{\mathrm{U}} + D_i$. Using the fact that both $\mathbf{H}_i(f) \triangleq \mathcal{F}\{h_i(t)\}$ and $\mathbf{W}_i(f) \triangleq \mathcal{F}\{w_i(t)\}$ are approximately constant over the frequencies of the NB signal, Appendix A shows that (11) can be reduced to

$$\mathbf{X}_i = k_{\mathrm{U}}\sqrt{E_{\mathrm{U}}}\,\mathbf{W}_i(-f_{\mathrm{U}}')\mathbf{H}_i(f_{\mathrm{N}})e^{-j2\pi f_{\mathrm{U}} D_i} \times \sum_{n=-\infty}^{\infty} a_{i,n}^{\mathrm{U}} e^{j\theta_{i,n}^{\mathrm{U}}} g(\widetilde{D}_{i,n}) e^{j2\pi f_{\mathrm{U}}' \widetilde{D}_{i,n}}, \tag{12}$$

with $f_{\mathrm{U}}' \triangleq f_{\mathrm{U}} - f_{\mathrm{N}}$. Note that effective range of the summation of n in (12) depends on the duration of the shaping pulse $g(t)$ relative to T_{U}. In effect, in the usual case where $g(t)$ decreases to 0 as $t \to \pm\infty$, the r.v.'s $g(\widetilde{D}_{i,n})$ become increasingly small since $|\widetilde{D}_{i,n}|$ grows as $|n|$ increases, and the sum in n can be truncated.

B. Distribution of the Aggregate UWB Interference

The distribution of the aggregate UWB interference $\mathbf{Y}$ plays an important role in the evaluation of the error probability of the victim link. In what follows, we characterize such distribution in two important scenarios: the $\mathcal{P}$-conditioned and $\mathcal{P}$-averaged cases.

1) $\mathcal{P}$-conditioned Interference Distribution: To derive the $\mathcal{P}$-conditioned distribution of the aggregate interference $\mathbf{Y}$ in (10), we approximate $\mathbf{X}_i$ in (12) by a circularly symmetric (CS) complex Gaussian r.v.,[11] such that

$$\mathbf{X}_i \sim \mathcal{N}_{\mathrm{c}}(0, 2V_X), \quad V_X \triangleq \mathbb{V}\{\mathrm{Re}\{\mathbf{X}_i\}\}. \tag{13}$$

The accuracy of this approximation is confirmed using both Kullback-Leibler (KL) divergence [47] in Table I, and error probability simulations in Section V. For simplicity, the table focuses on the worst case scenario by neglecting the noise term $\mathbf{N}$ in (8). The functions $f_{\mathrm{Re}\{\mathbf{X}_i\}}$ and $f_{\mathrm{Re}\{\mathbf{Z}\}}$ denote the p.d.f.'s without approximations, while $\widetilde{f}_{\mathrm{Re}\{\mathbf{X}_i\}}$ and $\widetilde{f}_{\mathrm{Re}\{\mathbf{Z}\}}$ denote the corresponding p.d.f.'s under the Gaussian approximation. We define $N_{\mathrm{p}} = T_{\mathrm{N}}/T_{\mathrm{U}}$ and $\mathsf{SIR} = k_{\mathrm{N}}^2 E_{\mathrm{N}}/k_{\mathrm{U}}^2 E_{\mathrm{U}}$. Note that the divergence $D(f_{\mathrm{Re}\{\mathbf{Z}\}} \parallel \widetilde{f}_{\mathrm{Re}\{\mathbf{Z}\}})$ is a r.v., since it depends on the particular realization of $\mathcal{P}$. The divergence values are obtained through Monte Carlo simulation with $T_{\mathrm{U}} = 0.5\,\mu\mathrm{s}$, $r_0 = 1\,\mathrm{m}$, $\lambda_{\mathrm{U}} = 0.1\,\mathrm{m}^{-2}$, and the remaining system parameters are described in Section V and Table II. We conclude that as N_{p} increases, $\mathbf{X}_i$ approaches a Gaussian r.v., since the number of summands (12) increases. Even for small values of N_{p} where $\mathbf{X}_i$ does not resemble a Gaussian r.v., what is important in error probability evaluation is the p.d.f. of the overall decision variable $\mathbf{Z}$, not of $\mathbf{X}_i$ itself.

[11]A r.v. $\mathbf{X}$ is said to be circularly symmetric if its p.d.f. $f_{\mathbf{X}}(\mathbf{x})$ depends only on $|\mathbf{x}|$.

The rightmost column of Table I shows that the p.d.f. of $\mathbf{Z}$ indeed remains essentially the same if the approximation in (13) is made.[12] This is also in agreement with [50], which shows that even the case of a single interferer (i.e., $\mathbf{Y}$ only has a single term), the Rayleigh fading affecting the desired signal mitigates the non-Gaussian characteristics of the interference. A detailed analysis of the interfering term can be found in [24]. In addition to KL divergence arguments, we also performed physical-level simulations of the network, without any approximations, to verify the validity of (13). In particular, Section V shows that the Gaussian approximation has a negligible effect on the overall error performance.

With the approximation in (13), the interference $\mathbf{Y}$ in (10) becomes a sum of independent CS Gaussian r.v.'s and is therefore a CS Gaussian r.v. with distribution given by[13]

$$\mathbf{Y} \overset{|\mathcal{P}}{\sim} \mathcal{N}_{\mathrm{c}}(0, 2AV_X), \tag{14}$$

where A is defined as

$$A \triangleq \sum_{i=1}^{\infty} \frac{e^{2\sigma_{\mathrm{U}} G_i}}{R_i^{2\nu_{\mathrm{U}}}}. \tag{15}$$

Note that since A in (15) depends on $\mathcal{P}$ (i.e., $\{R_i\}_{i=1}^{\infty}$ and $\{G_i\}_{i=1}^{\infty}$), it can be seen as a r.v. whose value is different for each realization of $\mathcal{P}$. Furthermore, Appendix B shows that the r.v. A has a *skewed stable distribution* [51] given by[14]

$$A \sim \mathcal{S}\left(\alpha_A = \frac{1}{\nu_{\mathrm{U}}},\ \beta_A = 1,\ \gamma_A = \pi\lambda_{\mathrm{U}} C_{1/\nu_{\mathrm{U}}}^{-1} e^{2\sigma_{\mathrm{U}}^2/\nu_{\mathrm{U}}^2}\right), \tag{16}$$

where $\nu_{\mathrm{U}} > 1$, and C_α is defined as

$$C_\alpha \triangleq \begin{cases} \frac{1-\alpha}{\Gamma(2-\alpha)\cos(\pi\alpha/2)}, & \alpha \neq 1, \\ \frac{2}{\pi}, & \alpha = 1. \end{cases} \tag{17}$$

This distribution is plotted in Fig. 2 for different values of ν and λ.

2) $\mathcal{P}$-averaged Interference Distribution: To derive such distribution, we first analyze the properties of $\mathbf{X}_i$ in (12). Typically, it is accurate to consider that $\varphi_i \triangleq \arg\{\mathbf{H}_i(f_{\mathrm{N}})\}$ has a $\mathcal{U}(0, 2\pi)$ distribution, independent of everything else. Then, we can rewrite (12) as $\mathbf{X}_i = \breve{\mathbf{X}}_i e^{j\varphi_i}$, where φ_i is independent of $\breve{\mathbf{X}}_i$; thus, $\mathbf{X}_i$ is CS. Furthermore, since different interferers i transmit independently, the r.v.'s $\mathbf{X}_i$ are i.i.d. in i.

Sums of the form of (10) belong to the class of *symmetric stable distributions* [51]. This is because the r.v.'s $\{R_i\}_{i=1}^{\infty}$ correspond to distances in a spatial Poisson process, and the $\{\mathbf{X}_i\}_{i=1}^{\infty}$ are i.i.d. with a CS distribution. Specifically,

[12]Note that when conditioned on $\mathcal{P}$ (i.e., $\{R_i\}_{i=1}^{\infty}$ and $\{G_i\}_{i=1}^{\infty}$), $\mathbf{Y}$ in (10) is a sum of the independent (but not identically distributed) r.v.'s $\{e^{\sigma_{\mathrm{U}} G_i}\mathbf{X}_i / R_i^{\nu_{\mathrm{U}}}\}_{i=1}^{\infty}$. It can be shown that in this case, the more general (Lindeberg) form of the central limit theorem [48] does not apply to $\mathbf{Y}$, due to the vanishing nature of the terms in the sum [49].

[13]We use $X \overset{|Y}{\sim}$ to denote the distribution of r.v. X conditioned on Y.

[14]We use $\mathcal{S}(\alpha, \beta, \gamma)$ to denote a real stable distribution with characteristic exponent $\alpha \in (0, 2]$, skewness $\beta \in [-1, 1]$, dispersion $\gamma \in [0, \infty)$, and location $\mu = 0$. The corresponding characteristic function is

$$\phi(w) = \begin{cases} \exp\left[-\gamma|w|^\alpha \left(1 - j\beta\,\mathrm{sign}(w)\tan\frac{\pi\alpha}{2}\right)\right], & \alpha \neq 1, \\ \exp\left[-\gamma|w|\left(1 + j\frac{2}{\pi}\beta\,\mathrm{sign}(w)\ln|w|\right)\right], & \alpha = 1. \end{cases}$$

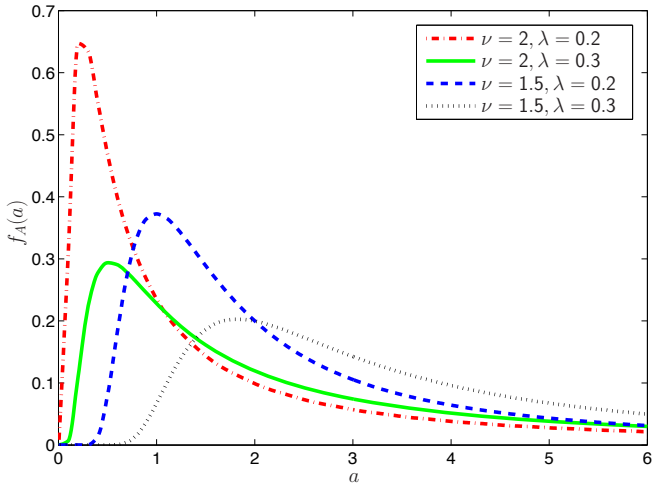

Fig. 2. Probability density function of A for different amplitude loss exponents ν and spatial densities λ ($\sigma_{\mathrm{dB}} = 3$).

Appendix C shows that $\mathbf{Y}$ has a CS complex stable distribution given by[15]

$$\mathbf{Y} \sim \mathcal{S}_{\mathrm{c}}\left(\alpha_{\mathbf{Y}} = \frac{2}{\nu_{\mathrm{U}}},\ \beta_{\mathbf{Y}} = 0,\right. \tag{18}$$
$$\left.\gamma_{\mathbf{Y}} = \pi\lambda_{\mathrm{U}} C_{2/\nu_{\mathrm{U}}}^{-1} e^{2\sigma_{\mathrm{U}}^2/\nu_{\mathrm{U}}^2} \mathbb{E}\left\{|\mathrm{Re}\{\mathbf{X}_i\}|^{2/\nu_{\mathrm{U}}}\right\}\right),$$

where $\nu_{\mathrm{U}} > 1$.

3) Discussion: The results of this section have to be interpreted carefully, because of the different types of conditioning involved. In the unconditional case, we let $\mathcal{P}$ be random, i.e., we let $\{R_i\}_{i=1}^{\infty}$ be the random outcomes of an underlying spatial Poisson process, and $\{G_i\}_{i=1}^{\infty}$ be the random shadowing affecting each UWB interferer. Then, the unconditional interference $\mathbf{Y}$ is *exactly* stable-distributed and given by (18). We note that (18) holds for a broad class of fading distributions, as long as the r.v.'s $\mathbf{X}_i$ in (10) are CS and i.i.d. in i. In the $\mathcal{P}$-conditioned case, the positions of the interferers are fixed. Then, A in (15) is also a fixed number, and the interference $\mathbf{Y}$ is *approximately* CS Gaussian with total variance $2AV_X$, as given in (14).

C. Error Probability

In the previous section, we determined the statistical distribution of the aggregate UWB interference at the output of a linear NB receiver. We now use such result to directly characterize the performance of the NB victim link subject to aggregate UWB interference and thermal noise, in terms of outage and average error probabilities.

1) Outage Error Probability: In this section, we analyze the error probability conditioned on a given realization $\mathcal{P}$ of the distances $\{R_i\}_{i=1}^{\infty}$ and shadowing $\{G_i\}_{i=1}^{\infty}$ associated with the UWB interferers, as well as on the shadowing G_0 of the NB victim link. We denote this conditional symbol error probability (SEP) by $P_{\mathrm{e}|G_0,\mathcal{P}}$.

To derive the conditional error probability, we employ the results of Section III-B1 for the $\mathcal{P}$-conditioned distribution of

[15]We use $\mathcal{S}_{\mathrm{c}}(\alpha, \beta = 0, \gamma)$ to denote a CS complex stable distribution with characteristic exponent α and dispersion γ, and whose characteristic function is $\phi(\mathbf{w}) = \exp(-\gamma|\mathbf{w}|^\alpha)$. Furthermore, the corresponding real and imaginary components are both $\mathcal{S}(\alpha, \beta = 0, \gamma)$.

TABLE I
ANALYSIS OF KULLBACK-LEIBLER DIVERGENCE (IN NATS).

		$D(f_{\mathrm{Re}\{\mathbf{X}_i\}} \parallel \widetilde{f}_{\mathrm{Re}\{\mathbf{X}_i\}})$	$\mathbb{E}_{\mathcal{P}}\{D(f_{\mathrm{Re}\{\mathbf{Z}\}} \parallel \widetilde{f}_{\mathrm{Re}\{\mathbf{Z}\}})\}$		
T_{N}	N_{p}	any SIR	$\mathsf{SIR} = -10\,\mathrm{dB}$	$\mathsf{SIR} = 0\,\mathrm{dB}$	$\mathsf{SIR} = 10\,\mathrm{dB}$
$0.1\,\mu\mathrm{s}$	0.2	2.961	0.0102	0.00512	0.00124
$1\,\mu\mathrm{s}$	2	0.213	0.00251	0.000332	0.000178
$5\,\mu\mathrm{s}$	10	0.164	0.00120	0.000145	0.0000571

the aggregate UWB interference $\mathbf{Y}$. Specifically, using (9) and (14), the received signal $\mathbf{Z}$ in (8) can be rewritten as

$$\mathbf{Z} = \frac{k_{\mathrm{N}}\alpha_0 e^{\sigma_{\mathrm{N}}G_0}}{r_0^{\nu_{\mathrm{N}}}}\sqrt{E_{\mathrm{N}}}\,a_0^{\mathrm{N}}e^{j\theta_0^{\mathrm{N}}} + \widetilde{\mathbf{N}}, \tag{19}$$

where

$$\widetilde{\mathbf{N}} = \mathbf{Y} + \mathbf{N} \overset{|\mathcal{P}}{\sim} \mathcal{N}_{\mathrm{c}}(0, 2AV_X + N_0), \tag{20}$$

and A was defined in (15). Our framework has thus reduced the analysis of NB communication in the presence of UWB network interference to a Gaussian problem, where the combined noise $\widetilde{\mathbf{N}}$ is Gaussian when conditioned on the location of the UWB interferers.

The corresponding error probability $P_{\mathrm{e}|G_0,\mathcal{P}}$ can be found by taking the well-known error probability expressions for coherent detection of linear modulations in the presence of AWGN and fast fading [42]–[46], but using $2AV_X + N_0$ instead of N_0 for the total noise variance. This substitution is valid for any linear modulation, allowing the traditional results to be extended to include the effect of UWB network interference. For the case where the NB transmitter employs an arbitrary signal constellation in the in-phase/quadrature (IQ) plane and the fading is Rayleigh-distributed, the conditional SEP is given by

$$P_{\mathrm{e}|G_0,\mathcal{P}} = \sum_{k=1}^{M} p_k \sum_{l\in\mathcal{B}_k} \frac{1}{2\pi} \times \int_0^{\phi_{k,l}} \left(1 + \frac{w_{k,l}}{4\sin^2(\theta+\psi_{k,l})}\eta_A\right)^{-1} d\theta \tag{21}$$

where

$$\eta_A = \frac{k_{\mathrm{N}}^2 e^{2\sigma_{\mathrm{N}}G_0}E_{\mathrm{N}}}{r_0^{2\nu_{\mathrm{N}}}(2AV_X + N_0)} \tag{22}$$

is the received signal-to-interference-plus-noise ratio (SINR), averaged over the fast fading; M is the NB constellation size; $\{p_k\}_{k=1}^{M}$ are the NB symbol probabilities; $\mathcal{B}_k$, $\phi_{k,l}$, $w_{k,l}$, and $\psi_{k,l}$ are the parameters that describe the geometry of the NB constellation, as depicted in [25, Fig. 10]; A is defined in (15) and distributed according to (16); and V_X is defined in (13). When the NB transmitter employs M-PSK and M-QAM modulations with equiprobable symbols, (21) is equivalent to[16]

$$P_{\mathrm{e}|G_0,\mathcal{P}}^{\mathrm{MPSK}} = \mathcal{I}\left(\frac{M-1}{M}\pi,\, \sin^2\left(\frac{\pi}{M}\right)\right) \tag{23}$$

and

$$P_{\mathrm{e}|G_0,\mathcal{P}}^{\mathrm{MQAM}} = 4\left(1 - \frac{1}{\sqrt{M}}\right)\cdot\mathcal{I}\left(\frac{\pi}{2},\, \frac{3}{2(M-1)}\right) - 4\left(1 - \frac{1}{\sqrt{M}}\right)^2\cdot\mathcal{I}\left(\frac{\pi}{4},\, \frac{3}{2(M-1)}\right) \tag{24}$$

where the integral $\mathcal{I}(x,g)$ is given by

$$\mathcal{I}(x,g) = \frac{1}{\pi}\int_0^x \left(1 + \frac{g}{\sin^2\theta}\eta_A\right)^{-1} d\theta. \tag{25}$$

In the general expression given in (21) and (22), the network interference is accounted for by the term $2AV_X$, where A depends on the spatial distribution of the UWB interferers and propagation characteristics of the medium, while V_X depends on the transmission characteristics of the UWB interferers. Since $2AV_X$ simply adds to N_0, we conclude that the effect of the interference on the error probability is simply an increase in the noise level, a fact which is intuitively satisfying. Furthermore, note that the modulation of the UWB interfering nodes only affects the term V_X, while the modulation of the NB link affects the *type* of error probability expression, leading to forms such as (23) or (24).

In our quasi-static model, the conditional error probability in (21) is seen to be a function of the slow-varying interferer positions and shadowing (i.e., G_0 and $\mathcal{P}$). Since these quantities are random, the error probability itself is a r.v. Then, with some probability, G_0 and $\mathcal{P}$ are such that the error probability of the victim link is above some target p^*. The system is said to be *in outage*, and the outage error probability is

$$P_{\mathrm{out}}^{\mathrm{e}} = \mathbb{P}_{G_0,\mathcal{P}}\{P_{\mathrm{e}|G_0,\mathcal{P}} > p^*\}. \tag{26}$$

In the case of slow-varying interferer positions, the outage error probability is a more meaningful metric than the error probability averaged over $\mathcal{P}$.

2) Average Error Probability: In this section, we average the error probability over all possible realizations of UWB interferer positions $\mathcal{P}$. We denote this average SEP by $P_{\mathrm{e}|G_0}$. We choose not to average out the shadowing G_0 affecting the NB transmitter, since we have assumed the NB transmitter is immobile at a deterministic distance r_0 from the NB receiver, and thus G_0 is slow-varying.

To derive the average error probability, we use the decomposition property of stable r.v.'s [51], which allows $\mathbf{Y}$ in (18) to be decomposed as

$$\mathbf{Y} = \sqrt{B}\mathbf{G}, \tag{27}$$

where B and $\mathbf{G}$ are independent r.v.'s such that

$$B \sim \mathcal{S}\left(\alpha_B = \frac{1}{\nu_{\mathrm{U}}},\, \beta_B = 1,\, \gamma_B = \cos\left(\frac{\pi}{2\nu_{\mathrm{U}}}\right)\right) \tag{28}$$

and

$$\mathbf{G} \sim \mathcal{N}_{\mathrm{c}}(0, 2V_G), \tag{29}$$

[16]In this paper, we implicitly assume that M-QAM employs a square signal constellation with $M = 2^n$ points (n even).

with

$$V_G = 2e^{2\sigma_{\rm U}^2/\nu_{\rm U}}\left[\pi\lambda_{\rm U}C_{2/\nu_{\rm U}}^{-1}\mathbb{E}\{|{\rm Re}\{\mathbf{X}_i\}|^{2/\nu_{\rm U}}\}\right]^{\nu_{\rm U}}. \quad (30)$$

Conditioning on the r.v. B, we then use (9) and (27) to rewrite the aggregate received signal $\mathbf{Z}$ in (8) as

$$\mathbf{Z} = \frac{k_{\rm N}\alpha_0 e^{\sigma_{\rm N}G_0}}{r_0^{\nu_{\rm N}}}\sqrt{E_{\rm N}}\,a_0^{\rm N}e^{j\theta_0^{\rm N}} + \widetilde{\mathbf{N}},$$

where

$$\widetilde{\mathbf{N}} = \sqrt{B}\mathbf{G} + \mathbf{N} \overset{|B}{\sim} \mathcal{N}_{\rm c}(0, 2BV_G + N_0). \quad (31)$$

Again, our framework has reduced the analysis of NB communication in the presence of UWB network interference to a Gaussian problem, where the combined noise $\widetilde{\mathbf{N}}$ is a Gaussian r.v. Note that this result was derived without resorting to approximations – in particular, the Gaussian approximation of (13) was not needed here. We merely used the decomposition property of symmetric stable r.v.'s.

The corresponding error probability $P_{{\rm e}|G_0}$ can be found by taking the error expressions for coherent detection in the presence of AWGN and fast fading, then using $2BV_G + N_0$ instead of N_0 for the total noise variance, and lastly (unlike in Section III-C1) averaging over the r.v. B. For the case where the NB transmitter employs an arbitrary signal constellation in the IQ-plane and the fading is Rayleigh-distributed, the average SEP is given by

$$P_{{\rm e}|G_0} = \sum_{k=1}^{M} p_k \sum_{l\in\mathcal{B}_k}\frac{1}{2\pi} \times \int_0^{\phi_{k,l}} \mathbb{E}_B\left\{\left(1 + \frac{w_{k,l}}{4\sin^2(\theta+\psi_{k,l})}\eta_B\right)^{-1}\right\} d\theta, \quad (32)$$

where

$$\eta_B = \frac{k_{\rm N}^2 e^{2\sigma_{\rm N}G_0}E_{\rm N}}{r_0^{2\nu_{\rm N}}(2BV_G + N_0)}; \quad (33)$$

B is distributed according to (28); V_G is given in (30); and the other parameters have the same meaning as in Section III-C1. For the special cases where the NB transmitter employs M-PSK and M-QAM modulations with equiprobable symbols, (32) reduces to (23) and (24), respectively, except the integral $\mathcal{I}(x,g)$ is now given by

$$\mathcal{I}(x,g) = \frac{1}{\pi}\int_0^x \mathbb{E}_B\left\{\left(1 + \frac{g}{\sin^2\theta}\eta_B\right)^{-1}\right\} d\theta. \quad (34)$$

IV. UWB Communication in the Presence of NB Interferers

A. Signals and Interference Models

In many practical scenarios, the signal in (2) transmitted by the ith NB interferer can be well modeled by a tone at frequency $f_{\rm N}$ [18], [22], i.e.,

$$s_i^{\rm N}(t) \approx \sqrt{2P_{\rm N}}\cos\left(2\pi f_{\rm N}(t - D_i)\right), \quad (35)$$

where $P_{\rm N} = E_{\rm N}/T_{\rm N}$ is the average power of each interferer, and D_i are i.i.d. time delays that account for the asynchronism between the NB transmitters. The aggregate signal $z(t)$ at the UWB receiver can be written as

$$z(t) = d(t) + y(t) + n(t),$$

where $d(t) = \left[\sqrt{2E_{\rm U}}\,a_0^{\rm U}w(t)\cos\left(2\pi f_{\rm U}t + \theta_0^{\rm U}\right)\right] * \widetilde{h}_0^{\rm U}(t)$ is the desired signal from the UWB transmitter corresponding to symbol $n = 0$;[17] $y(t) = \sum_{i=1}^{\infty} s_i^{\rm N}(t) * \widetilde{h}_i^{\rm N}(t)$ is the aggregate network interference; and $n(t)$ is the AWGN with two-sided PSD $N_0/2$, and independent of $y(t)$. By performing the indicated convolutions, we can further express the desired signal as

$$d(t) = \frac{k_{\rm U}e^{\sigma_{\rm U}G_0}}{r_0^{\nu_{\rm U}}}\sqrt{2E_{\rm U}}\,a_0^{\rm U} \times \sum_{q=1}^{L} h_q w(t - t_q)\cos\left(2\pi f_{\rm U}(t - t_q) + \theta_0^{\rm U}\right), \quad (36)$$

and the aggregate interference as

$$y(t) = k_{\rm N}\sqrt{2P_{\rm N}}\sum_{i=1}^{\infty}\frac{e^{\sigma_{\rm N}G_i}}{R_i^{\nu_{\rm N}}}\alpha_i\cos\left(2\pi f_{\rm N}(t - D_i) + \phi_i\right). \quad (37)$$

The desired UWB signal in (36) is subject to both aggregate NB interference and AWGN. If only AWGN is present, the optimum receiver consists of a matched filter (MF) or, equivalently, a correlator. In the presence of multipath, this MF is realized adaptively as the well-known Rake receiver. In this case, the UWB receiver demodulates the aggregate signal by projecting $z(t)$ onto the function

$$\mathbf{\Psi}(t) = \sqrt{2}\sum_{q=1}^{L} h_q w(t - t_q)e^{-j2\pi f_{\rm U}(t - t_q)}. \quad (38)$$

Defining $\mathbf{Z} = \int_{-\infty}^{+\infty} z(t)\mathbf{\Psi}(t)dt$ we can write[18]

$$\mathbf{Z} = a_0^{\rm U}e^{j\theta_0^{\rm U}}\frac{k_{\rm U}e^{\sigma_{\rm U}G_0}}{r_0^{\nu_{\rm U}}}\sqrt{E_{\rm U}}\alpha_{{\rm U}|\mathbf{h}}^2 + \mathbf{Y} + \mathbf{N} \quad (39)$$

where $\alpha_{{\rm U}|\mathbf{h}}^2 \triangleq \sum_{q=1}^{L} h_q^2$ with $\mathbf{h} = (h_1, h_2, \ldots, h_L)$ denoting the instantaneous path gains, and the distribution of $\mathbf{N}$ is given by

$$\mathbf{N} \sim \mathcal{N}_{\rm c}\left(0, N_0\alpha_{{\rm U}|\mathbf{h}}^2\right). \quad (40)$$

Furthermore, $\mathbf{Y} = \int_{-\infty}^{+\infty} y(t)\mathbf{\Psi}(t)dt$ can be expressed as

$$\mathbf{Y} = \sum_{i=1}^{\infty}\frac{e^{\sigma_{\rm N}G_i}\mathbf{X}_i}{R_i^{\nu_{\rm N}}}, \quad (41)$$

where

$$\mathbf{X}_i = 2k_{\rm N}\sqrt{P_{\rm N}}\,\alpha_i\sum_{q=1}^{L}h_q \times \int_{-\infty}^{+\infty}\cos\left(2\pi f_{\rm N}(t + t_q) + \phi_i\right)w(t)e^{-j2\pi f_{\rm U}t}dt. \quad (42)$$

[17] To derive the error probability of the UWB victim link, we only need to analyze a single UWB symbol, since we assume that pulses satisfy the Nyquist criterion (or introduce, in any case, negligible intersymbol interference) and we consider perfect synchronization with the desired UWB signal.

[18] We consider that the multipath is resolvable and the channel is perfectly estimated. Moreover, distortion (such as that caused by antennas in UWB systems) can be taken into account by considering $w(t)$ to be the received waveform.

With a slight abuse of notation, the phase terms $-2\pi f_{\mathrm{N}} D_i$ were absorbed by the random phases ϕ_i.

We define the frequency response of the victim's UWB channel in (5) as

$$\mathbf{H}_{\mathrm{U}|\mathbf{h},\mathbf{t}}(f) \triangleq \mathcal{F}\{h_{\mathrm{U}}(t)\} = \sum_{q=1}^{L} h_q e^{-j2\pi f t_q} \tag{43}$$

with $\mathbf{t} = (t_1, t_2, \ldots, t_L)$ denoting the vector of instantaneous path delays. Appendix D shows that (42) can be reduced to

$$\mathbf{X}_i = k_{\mathrm{N}} \sqrt{P_{\mathrm{N}}}\, \alpha_i e^{j\phi_i} \mathbf{W}(f_{\mathrm{U}} - f_{\mathrm{N}}) \mathbf{H}^{*}_{\mathrm{U}|\mathbf{h},\mathbf{t}}(f_{\mathrm{N}}), \tag{44}$$

where $\mathbf{W}(f) \triangleq \mathcal{F}\{w(t)\}$. Note from (43) that $\mathbf{H}_{\mathrm{U}|\mathbf{h},\mathbf{t}}(f_{\mathrm{N}})$ depends on the instantaneous CIR $h_{\mathrm{U}}(t)$ through $\mathbf{h}$ and $\mathbf{t}$.

B. Distribution of the Aggregate NB Interference

The distribution of the aggregate NB interference $\mathbf{Y}$ plays an important role in the evaluation of the error probability of the victim link. In what follows, we characterize such distribution in two important scenarios: the $\mathcal{P}$-conditioned and $\mathcal{P}$-averaged cases. Unlike Section III-B, here the interference $\mathbf{Y}$ also depends on the CIR of the victim's UWB channel through $\mathbf{H}_{\mathrm{U}|\mathbf{h},\mathbf{t}}(f_{\mathrm{N}})$. Therefore, all the interference distributions derived in this section are conditioned on $\mathbf{h}$ and $\mathbf{t}$, which we will later use in deriving the error performance. In what follows, we consider the symbol waveform $w(t)$ of the UWB victim to be deterministic, which in the context of the IR signal in (3), corresponds to considering the sequences $\{c_k^{\mathrm{DS}}\}$ and $\{c_k^{\mathrm{TH}}\}$ to be deterministic. This is a natural assumption when the spreading sequences of the victim UWB receiver are deterministically known.

1) $\mathcal{P}$-conditioned Interference Distribution: To derive the $\mathcal{P}$-conditioned distribution of the aggregate interference $\mathbf{Y}$ in (41), we need the exact distribution of the $\mathbf{X}_i$ in (44). The term $\alpha_i e^{j\phi_i}$ is the product of a Rayleigh r.v. and a complex unitary vector with phase $\phi_i \sim \mathcal{U}(0, 2\pi)$, and thus $\mathbf{X}_i$ is CS complex Gaussian when conditioned on $\mathbf{h}$ and $\mathbf{t}$. This can be summarized in the following equation:

$$\mathbf{X}_i \overset{|\mathbf{h},\mathbf{t}}{\sim} \mathcal{N}_{\mathrm{c}}(0, 2V_{X|\mathbf{h},\mathbf{t}}), \quad V_{X|\mathbf{h},\mathbf{t}} \triangleq \mathbb{V}\{\mathrm{Re}\{\mathbf{X}_i\}|\mathbf{h},\mathbf{t}\}. \tag{45}$$

Hence, $\mathbf{Y}$ in (41) becomes a sum of independent CS Gaussian r.v.'s and is therefore a CS Gaussian r.v. with distribution given by

$$\mathbf{Y} \overset{|\mathcal{P},\mathbf{h},\mathbf{t}}{\sim} \mathcal{N}_{\mathrm{c}}(0, 2AV_{X|\mathbf{h},\mathbf{t}}), \tag{46}$$

where A is defined similarly to (15) as

$$A \triangleq \sum_{i=1}^{\infty} \frac{e^{2\sigma_{\mathrm{N}} G_i}}{R_i^{2\nu_{\mathrm{N}}}}. \tag{47}$$

Using an argument analogous to Appendix B, we can show that A has a skewed stable distribution given by

$$A \sim \mathcal{S}\left(\alpha_A = \frac{1}{\nu_{\mathrm{N}}},\ \beta_A = 1,\ \gamma_A = \pi\lambda_{\mathrm{N}} C^{-1}_{1/\nu_{\mathrm{N}}} e^{2\sigma_{\mathrm{N}}^2/\nu_{\mathrm{N}}^2}\right), \tag{48}$$

where $\nu_{\mathrm{N}} > 1$. This distribution is plotted in Fig. 2 for different values of ν and λ.

2) $\mathcal{P}$-averaged Interference Distribution: Conditioned on $\mathbf{h}$ and $\mathbf{t}$, the r.v.'s $\mathbf{X}_i$ are CS complex Gaussian and i.i.d. in i, since different interferers i transmit independently. Therefore, using an argument analogous to Appendix C, we can show that $\mathbf{Y}$ has a CS complex stable distribution given by

$$\mathbf{Y} \overset{|\mathbf{h},\mathbf{t}}{\sim} \mathcal{S}_{\mathrm{c}}\Bigg(\alpha_{\mathbf{Y}} = \frac{2}{\nu_{\mathrm{N}}},\ \beta_{\mathbf{Y}} = 0, \tag{49}$$

$$\gamma_{\mathbf{Y}} = \pi\lambda_{\mathrm{N}} C^{-1}_{2/\nu_{\mathrm{N}}} e^{2\sigma_{\mathrm{N}}^2/\nu_{\mathrm{N}}^2}\, \mathbb{E}\left\{|\mathrm{Re}\{\mathbf{X}_i\}|^{2/\nu_{\mathrm{N}}}|\mathbf{h},\mathbf{t}\right\}\Bigg),$$

where $\nu_{\mathrm{N}} > 1$.

C. Error Probability

In the previous section, we determined the statistical distribution of the aggregate NB interference at the output of a UWB Rake receiver. We now use such result to directly characterize the performance of the UWB victim link, when subject to aggregate NB interference and thermal noise, in terms of outage and average error probabilities.

1) Outage Error Probability: To derive the conditional error probability $P_{\mathrm{e}|G_0,\mathcal{P}}$, we employ the results of Section IV-B1 for the $\mathcal{P}$-conditioned distribution of the aggregate NB interference $\mathbf{Y}$. Specifically, using (40) and (46), the received signal $\mathbf{Z}$ in (39) can be rewritten as

$$\mathbf{Z} = a_0^{\mathrm{U}} e^{j\theta_0^{\mathrm{U}}} \frac{k_{\mathrm{U}} e^{\sigma_{\mathrm{U}} G_0}}{r_0^{\nu_{\mathrm{U}}}} \sqrt{E_{\mathrm{U}}}\, \alpha^2_{\mathrm{U}|\mathbf{h}} + \widetilde{\mathbf{N}}, \tag{50}$$

where

$$\widetilde{\mathbf{N}} = \mathbf{Y} + \mathbf{N} \overset{|\mathcal{P},\mathbf{h},\mathbf{t}}{\sim} \mathcal{N}_{\mathrm{c}}\left(0, 2AV_{X|\mathbf{h},\mathbf{t}} + N_0 \alpha^2_{\mathrm{U}|\mathbf{h}}\right), \tag{51}$$

and A was defined in (47). From (44), the term $V_{X|\mathbf{h},\mathbf{t}}$ is given by

$$V_{X|\mathbf{h},\mathbf{t}} = \frac{k_{\mathrm{N}}^2}{2} P_{\mathrm{N}} \left|\mathbf{W}(f_{\mathrm{U}} - f_{\mathrm{N}})\right|^2 \left|\mathbf{H}_{\mathrm{U}|\mathbf{h},\mathbf{t}}(f_{\mathrm{N}})\right|^2. \tag{52}$$

When conditioned on the nodes' shadowing and position (G_0 and $\mathcal{P}$), as well as on the instantaneous CIR ($\mathbf{h}$ and $\mathbf{t}$), the error probability $P_{\mathrm{e}|\mathbf{h},\mathbf{t},G_0,\mathcal{P}}$ for the case when the UWB transmitter employs an arbitrary signal constellation in the IQ-plane can be written as

$$P_{\mathrm{e}|\mathbf{h},\mathbf{t},G_0,\mathcal{P}} = \sum_{k=1}^{M} p_k \sum_{l\in\mathcal{B}_k} \frac{1}{2\pi} \tag{53}$$

$$\times \int_0^{\phi_{k,l}} \exp\left(-\frac{w_{k,l}}{4\sin^2(\theta + \psi_{k,l})} \tilde{\eta}_{\mathbf{h},\mathbf{t},G_0,\mathcal{P}}\right) d\theta,$$

where

$$\tilde{\eta}_{\mathbf{h},\mathbf{t},G_0,\mathcal{P}} = \frac{k_{\mathrm{U}}^2 \alpha^2_{\mathrm{U}|\mathbf{h}}\, e^{2\sigma_{\mathrm{U}} G_0}}{r_0^{2\nu_{\mathrm{U}}} \left(\frac{N_0}{E_{\mathrm{U}}} + \frac{2V_{X|\mathbf{h},\mathbf{t}}}{P_{\mathrm{U}} T_{\mathrm{U}} \alpha^2_{\mathrm{U}|\mathbf{h}}} A\right)}; \tag{54}$$

$P_{\mathrm{U}} = E_{\mathrm{U}}/T_{\mathrm{U}}$ denotes the transmitted power, and the other parameters have the same meaning as in Section III-C1.

The next step is to perform expectations of $P_{\mathrm{e}|\mathbf{h},\mathbf{t},G_0,\mathcal{P}}$ over r.v.'s $\mathbf{h}$ and $\mathbf{t}$, to obtain the average performance over all the possible CIRs $h_{\mathrm{U}}(t)$. The contribution of the interference in (54) depends on the instantaneous CIR of the desired signal, which makes the closed-form evaluation of $\mathbb{E}_{\mathbf{h},\mathbf{t}}\{P_{\mathrm{e}|\mathbf{h},\mathbf{t},G_0,\mathcal{P}}\}$ cumbersome and difficult. According to [22], we can proceed in two steps: first, perform the average over the time delays $\mathbf{t}$

for fixed path gains $\mathbf{h}$, and then average over $\mathbf{h}$, i.e., $P_{\mathrm{e}|G_0,\mathcal{P}} = \mathbb{E}_{\mathbf{h}}\{\mathbb{E}_{\mathbf{t}}\{P_{\mathrm{e}|\mathbf{h},\mathbf{t},G_0,\mathcal{P}}\}\}$. In this case, the inner expectation involves only the r.v. $\mathbf{t}$ through the function $|\mathbf{H}_{\mathrm{U}|\mathbf{h},\mathbf{t}}(f_{\mathrm{N}})|^2$. Therefore, without loss of generality, in the following we define a r.v. $\xi \triangleq |\mathbf{H}_{\mathrm{U}|\mathbf{h},\mathbf{t}}(f_{\mathrm{N}})|^2$ that depends on r.v. $\mathbf{t}$ with fixed (but arbitrary) $\mathbf{h}$. Hence, $P_{\mathrm{e}|\mathbf{h},G_0,\mathcal{P}} = \mathbb{E}_{\xi}\{\check{P}(\xi)\}$ where $\check{P}(\xi)$ has the same form as (53) with $\check{\eta}(\xi)$ instead of $\tilde{\eta}_{\mathbf{h},\mathbf{t},G_0,\mathcal{P}}$, where

$$\check{\eta}(\xi) = \frac{k_{\mathrm{U}}^2 \alpha_{\mathrm{U}|\mathbf{h}}^2 \, e^{2\sigma_{\mathrm{U}} G_0}}{r_0^{2\nu_{\mathrm{U}}} \left(\frac{N_0}{E_{\mathrm{U}}} + \frac{k_{\mathrm{N}}^2 P_{\mathrm{N}}}{P_{\mathrm{U}}} \frac{|\mathbf{W}(f_{\mathrm{U}} - f_{\mathrm{N}})|^2}{T_{\mathrm{U}}} \frac{\xi}{\alpha_{\mathrm{U}|\mathbf{h}}^2} A \right)}. \tag{55}$$

The expectation of $\check{P}(\xi)$ over the r.v. ξ can be conveniently approximated by means of *perturbation theory* [52], [53] without requiring integration. In fact, in [22] we prove that by expanding $\check{P}(\xi)$ in terms of central differences up to the third order and approximating the moments of ξ, we can obtain an accurate approximation of $P_{\mathrm{e}|\mathbf{h},G_0,\mathcal{P}}$ in closed-form. Specifically, the average SEP over the r.v. $\mathbf{t}$ can be written in the form

$$P_{\mathrm{e}|\mathbf{h},G_0,\mathcal{P}} \simeq \sum_{j=1}^{N} \rho_j \, \check{P}\left(\sigma_j \, \alpha_{\mathrm{U}|\mathbf{h}}^2\right), \tag{56}$$

where ρ_j and σ_j are weights, and N is the number of terms in the expansion. Considering the third-order expansion, we have $N = 4$ terms and the weights given by [22]

$$\boldsymbol{\rho} = \left(\frac{1}{6} + b,\, \frac{2}{3},\, \frac{1}{6} - 2b,\, b\right),$$
$$\boldsymbol{\sigma} = \left(0,\, 1,\, 1 + \sqrt{3\,a},\, 1 + 2\sqrt{3\,a}\right),$$

where

$$a = 1 - \Upsilon_2,$$
$$b = \frac{1 - 3\Upsilon_2 + 2\Upsilon_3}{18\sqrt{3}(1 - \Upsilon_2)^{3/2}},$$

are functions of Υ_2 and Υ_3 that depend only on the normalized PDP of the channel, i.e., $\Upsilon_2 = \sum_{q=1}^{L} \Omega_q^2$ and $\Upsilon_3 = \sum_{q=1}^{L} \Omega_q^3$, with $\Omega_q = \mathbb{E}\{h_q^2\}$.

Note that (56) is a function of $\mathbf{h}$ through the term $\alpha_{\mathrm{U}|\mathbf{h}}^2$, and hence the outer expectation $P_{\mathrm{e}|G_0,\mathcal{P}} = \mathbb{E}_{\mathbf{h}}\{P_{\mathrm{e}|\mathbf{h},G_0,\mathcal{P}}\}$ can be written as the expectation of (56) with respect to $\alpha_{\mathrm{U}|\mathbf{h}}^2$. The distribution of $\alpha_{\mathrm{U}|\mathbf{h}}^2$ depends on the type of channel. Considering independent paths $\{h_q\}_{q=1}^{L}$, it is possible to derive the expectation of (56) over $\mathbf{h}$ as

$$P_{\mathrm{e}|G_0,\mathcal{P}} = \sum_{k=1}^{M} p_k \sum_{l \in \mathcal{B}_k} \frac{1}{2\pi} \int_0^{\phi_{k,l}} \sum_{j=1}^{N} \rho_j \times \prod_{q=1}^{L} M_{h_q^2}\left(\frac{w_{k,l}}{4\sin^2(\theta + \psi_{k,l})} \eta_{G_0,\mathcal{P}}(\sigma_j)\right) d\theta, \tag{57}$$

where

$$\eta_{G_0,\mathcal{P}}(\sigma_j) = \frac{k_{\mathrm{U}}^2 e^{2\sigma_{\mathrm{U}} G_0}}{r_0^{2\nu_{\mathrm{U}}} \frac{N_0}{E_{\mathrm{U}}} \left(1 + \frac{k_{\mathrm{N}}^2 P_{\mathrm{N}} T_{\mathrm{U}}}{N_0} \cdot \frac{|\mathbf{W}(f_{\mathrm{U}} - f_{\mathrm{N}})|^2}{T_{\mathrm{U}}} \cdot A \cdot \sigma_j\right)} \tag{58}$$

is the SINR as a function of the signal-to-noise ratio $\mathsf{SNR} = k_{\mathrm{U}}^2 E_{\mathrm{U}}/N_0$ and the interference-to-noise ratio $\mathsf{INR} = k_{\mathrm{N}}^2 P_{\mathrm{N}} T_{\mathrm{U}}/N_0$, and $M_X(s) = \mathbb{E}\{e^{-sX}\}$ is the moment generating function (m.g.f.) of the r.v. X. Note that (58) depends only on the difference between the carrier frequencies f_{N} and f_{U}. For UWB channels, it has been shown [4] that the amplitude distribution of the resolved multipaths can be modeled by a Nakagami-m distribution. As a result, considering independent Nakagami distributed paths $|h_q|$ with average power Ω_q and Nakagami parameter m_q, the corresponding m.g.f. can be expressed as $M_{h_q^2}(s) = \left(1 + s\frac{\Omega_q}{m_q}\right)^{-m_q}$.

For the special cases where the UWB transmitter employs M-PSK and M-QAM modulations with equiprobable symbols, (57) reduces to (23) and (24), respectively, except the integral $\mathcal{I}(x,g)$ is now given by

$$\mathcal{I}(x,g) = \frac{1}{\pi} \int_0^x \sum_{j=1}^{N} \rho_j \prod_{q=1}^{L} M_{h_q^2}\left(\frac{g}{\sin^2\theta} \cdot \eta_{G_0,\mathcal{P}}(\sigma_j)\right) d\theta\,. \tag{59}$$

As before, the corresponding outage error probability can be defined as $P_{\mathrm{out}}^{\mathrm{e}} = \mathbb{P}_{G_0,\mathcal{P}}\{P_{\mathrm{e}|G_0,\mathcal{P}} > p^*\}$.

2) Average Error Probability: To derive the average error probability $P_{\mathrm{e}|G_0}$, we could perform a decomposition of the stable r.v. $\mathbf{Y}$ similar to (27). Unfortunately, in this case the calculation of the moment $\mathbb{E}\{|\mathrm{Re}\{\mathbf{X}_i\}|^{2/\nu_{\mathrm{N}}}|\mathbf{h},\mathbf{t}\}$ is quite cumbersome, and is not useful in evaluating the expectation of $P_{\mathrm{e}|\mathbf{h},\mathbf{t},G_0,\mathcal{P}}$ over $\mathbf{h}$ and $\mathbf{t}$. Therefore, a more straightforward way to compute the average SEP is to directly average (57) over the r.v. A as $P_{\mathrm{e}|G_0} = \mathbb{E}_A\{P_{\mathrm{e}|G_0,\mathcal{P}}\}$.

V. Numerical Results

We now particularize the general analysis developed in the previous sections, using a simple case study. We consider two specific scenarios: 1) a BPSK NB victim link subject to DS-BPAM UWB interferers, and 2) a DS-BPAM UWB victim link subject to NB BPSK interferers.

Considering DS-BPAM UWB interferers, the signal $s_i^{\mathrm{U}}(t)$ transmitted by the ith interferer in (1) becomes

$$s_i^{\mathrm{U}}(t) = \sqrt{2E_{\mathrm{U}}} \sum_n a_{i,n}^{\mathrm{U}} w_i(t - nN_{\mathrm{s}}T_{\mathrm{f}} - D_i) \cos\left(2\pi f_{\mathrm{U}}(t - D_i)\right),$$

where the unit-energy waveform $w_i(t)$ for each bit is

$$w_i(t) = \sum_{k=0}^{N_{\mathrm{s}}-1} c_{i,k}\, p(t - kT_{\mathrm{f}}).$$

In these equations, N_{s} is the number of monocycles required to transmit a single information bit $a_{i,n}^{\mathrm{U}} \in \{-1, 1\}$; $p(t)$ is the transmitted monocycle shape, with energy $1/N_{\mathrm{s}}$; T_{f} is the monocycle repetition time (frame length), related to the bit duration by $T_{\mathrm{U}} = N_{\mathrm{s}}T_{\mathrm{f}}$; and $\{c_{i,k}\}_{k=0}^{N_{\mathrm{s}}-1}$ is the spreading sequence, with $c_{i,k} \in \{-1, 1\}$. As in [2], we choose $p(t)$ to be the second derivative of a Gaussian monocycle,

$$p(t) = \sqrt{\frac{8}{3\tau_{\mathrm{p}} N_{\mathrm{s}}}} \left(1 - 4\pi\left(\frac{t}{\tau_{\mathrm{p}}}\right)^2\right) \exp\left(-2\pi\left(\frac{t}{\tau_{\mathrm{p}}}\right)^2\right),$$

where τ_{p} is the monocycle duration parameter.

Concerning the UWB propagation characteristics, we consider that the multipath fading channel in (5) is composed of L independent Nakagami-distributed paths having random

TABLE II
SYSTEM PARAMETERS USED IN NUMERICAL RESULTS.

	UWB systems	NB systems
Signals	DS-BPAM	BPSK
	$T_{\mathrm{U}} = 0.8\,\mu\mathrm{s}$	$T_{\mathrm{N}} = 1\,\mu\mathrm{s}$
	$f_{\mathrm{U}} = 4500\,\mathrm{MHz}$	$f_{\mathrm{N}} = 5010\,\mathrm{MHz}$
	$\tau_{\mathrm{p}} = 2\,\mathrm{ns}$	square $g(t)$
	$N_{\mathrm{s}} = 16$	
	$c_k^{\mathrm{DS}} = (-1)^k$	
Propagation	$\nu_{\mathrm{U}} = 2$	$\nu_{\mathrm{N}} = 2$
	$\sigma_{\mathrm{U,dB}} = 3$ (victim)	$\sigma_{\mathrm{N,dB}} = 4, 6, 8$ (interferers)
	$\sigma_{\mathrm{U,dB}} = 4, 6, 8$ (interferers)	$\sigma_{\mathrm{N,dB}} = 3$ (victim)
	Frequency-selective	Frequency-flat (Rayleigh)
	$L = 8$	
	$\epsilon_{\mathrm{p}} = 3$	
	$m_1 = 3$	
	$\epsilon_{\mathrm{m}} = 4$	

delays and an exponential PDP given by [4], [22]

$$\Omega_q = \frac{e^{1/\epsilon_{\mathrm{p}}} - 1}{1 - e^{-L/\epsilon_{\mathrm{p}}}} e^{-q/\epsilon_{\mathrm{p}}}, \quad q = 1, \ldots, L \tag{60}$$

where ϵ_{p} is a decay constant that controls the multipath dispersion. We also consider different Nakagami parameters for each path according to [22]

$$m_q = m_1 e^{-(q-1)/\epsilon_{\mathrm{m}}}, \quad q = 1, \ldots, L \tag{61}$$

where ϵ_{m} controls the decay of the m-parameters. Table II summarizes the system parameters used for all the numerical results.

We also compare our semi-analytical plots with the corresponding simulations. For the *semi-analytical plots*, we resort to a hybrid method where we employ the analytical expressions for $P_{\mathrm{out}}^{\mathrm{e}}$ and $P_{\mathrm{e}|G_0}$ given in Sections III and IV, and perform a Monte Carlo simulation of the stable r.v.'s A and B according to [54]. To validate these semi-analytical results, we resort to *physical-level simulations* of the system. Specifically, we simulate 10^5 instantiations of the position and shadowing of the interferers, over a circular area with radius 10^3 m. For the determination of average and outage error probabilities, we simulate 10^6 bits per node and instantiation. It will be apparent shortly that the semi-analytical plots are in good agreement with the physical-level simulations, suggesting that the expressions derived in the paper eliminate the need for physical-level simulation in order to obtain the error performance.

Figures 3(a) and (b) quantify the error performance of the BPSK NB victim link, subject to DS-BPAM UWB interference and noise. For this purpose, we define the normalized SNR of the NB link as $\mathsf{SNR} = k_{\mathrm{N}}^2 E_{\mathrm{N}}/N_0$, and the normalized INR as $\mathsf{INR} = k_{\mathrm{U}}^2 E_{\mathrm{U}}/N_0$.[19] We conclude that the error performance at a fixed SNR deteriorates as λ_{U} or the INR increase. This is expected because as the spatial density or transmitted energy of the UWB interferers increase, the aggregate interference at the NB victim receiver becomes stronger.

It is important to note that in a practical scenario it is possible to encounter INR values as high as $20-50$ dB. In fact, according to the IEEE 802.15.4a channel model, the term k_{U}^2 in $\mathsf{INR} = k_{\mathrm{U}}^2 E_{\mathrm{U}}/N_0$ can vary from -43.9 dB in the CM5 channel (LOS outdoor) to -73 dB in CM6 channel (NLOS outdoor); a typical value of P_{U} is -10 dBm (according to restrictions imposed by PSD masks); and a typical value of N_0 is -194 dBW/Hz (considering $N_0 = K_{\mathrm{B}} T_0 F$, where K_{B} is the Boltzmann constant, $T_0 = 290$ K, and $F = 10$ dB is the noise figure). Therefore, in this scenario, Fig. 3(a) shows that for $\mathsf{INR} = 50$ dB, $\mathsf{SNR} = 30$ dB, and $\lambda_{\mathrm{U}} = 0.1\,\mathrm{m}^{-2}$, the NB victim link experiences at least 1% outage. Similarly, Figure 3(b) shows that for $\mathsf{INR} = 40$ dB, $\mathsf{SNR} = 20$ dB, and $\lambda_{\mathrm{U}} = 0.1\,\mathrm{m}^{-2}$, the NB victim link experiences an average BEP greater than 10^{-2}. Depending on the application, such error performance could be non-satisfactory. Regarding the density of UWB nodes considered, $\lambda_{\mathrm{U}} = 0.1\,\mathrm{m}^{-2}$, it can be can easily reached in a suburban area by unregulated UWB devices. Therefore, despite the PSD limits imposed to UWB systems in attempt to protect existing communications, the effect of the aggregate UWB interference on NB systems can be significant in practice, and must be taken into account when considering coexistence.

Figures 4(a) and (b) quantify the error performance of a DS-BPAM victim link, subject to NB interference and noise, and illustrate its dependence on the various parameters involved, such as the $\mathsf{SNR} = k_{\mathrm{U}}^2 E_{\mathrm{U}}/N_0$, $\mathsf{INR} = k_{\mathrm{N}}^2 P_{\mathrm{N}} T_{\mathrm{U}}/N_0$, and interferer density λ_{N}. Again, we observe that the error performance at a fixed SNR deteriorates as λ_{N} or INR increase.

In this configuration, it is also possible in practice to encounter INR values as high as $50-70$ dB. In fact, the term k_{N}^2 in $\mathsf{INR} = k_{\mathrm{N}}^2 E_{\mathrm{N}}/N_0$ can be of the order of -50 to -70 dB

[19] Since E_{N} corresponds to the average transmitted symbol energy of the NB victim link, then $k_{\mathrm{N}}^2 E_{\mathrm{N}}$ can be interpreted as the average symbol energy measured 1 m away from the NB transmitter. An analogous interpretation applies to $k_{\mathrm{U}}^2 E_{\mathrm{U}}$.

$$\mathbf{X}_i = k_{\mathrm{U}}\sqrt{2E_{\mathrm{U}}}\sum_{n=-\infty}^{\infty} a_{i,n}^{\mathrm{U}} \int_{-\infty}^{+\infty} \left\{ \left[w_i(t-\widetilde{D}_{i,n}) \cos\left(2\pi f_{\mathrm{U}}(t-D_i)+\theta_{i,n}^{\mathrm{U}}\right)\right] * h_i(t) \right\} \times \sqrt{2} g(t) e^{-j2\pi f_{\mathrm{N}} t} dt$$

$$= k_{\mathrm{U}}\sqrt{E_{\mathrm{U}}}\sum_{n=-\infty}^{\infty} a_{i,n}^{\mathrm{U}} \left[e^{j\theta_{i,n}^{\mathrm{U}}} e^{-j2\pi f_{\mathrm{U}} D_i} \int_{-\infty}^{+\infty} \mathbf{W}_i(f-f_{\mathrm{U}}) \mathbf{H}_i(f) \mathbf{G}^*(f-f_{\mathrm{N}}) e^{-j2\pi(f-f_{\mathrm{U}})\widetilde{D}_{i,n}} df \right.$$

$$\left. + e^{-j\theta_{i,n}^{\mathrm{U}}} e^{j2\pi f_{\mathrm{U}} D_i} \int_{-\infty}^{+\infty} \mathbf{W}_i(f+f_{\mathrm{U}}) \mathbf{H}_i(f) \mathbf{G}^*(f-f_{\mathrm{N}}) e^{-j2\pi(f+f_{\mathrm{U}})\widetilde{D}_{i,n}} df \right] \tag{62}$$

$$= k_{\mathrm{U}}\sqrt{E_{\mathrm{U}}} \mathbf{H}_i(f_{\mathrm{N}}) \sum_{n=-\infty}^{\infty} a_{i,n}^{\mathrm{U}} \left[e^{j\theta_{i,n}^{\mathrm{U}}} e^{-j2\pi f_{\mathrm{U}} D_i} e^{j2\pi f_{\mathrm{U}} \widetilde{D}_{i,n}} \mathbf{W}_i(f_{\mathrm{N}}-f_{\mathrm{U}}) \right.$$

$$\left. + \underbrace{e^{-j\theta_{i,n}^{\mathrm{U}}} e^{j2\pi f_{\mathrm{U}} D_i} e^{-j2\pi f_{\mathrm{U}} \widetilde{D}_{i,n}} \mathbf{W}_i(f_{\mathrm{N}}+f_{\mathrm{U}})}_{=0} \right] \int_{-\infty}^{+\infty} \mathbf{G}^*(f-f_{\mathrm{N}}) e^{-j2\pi f \widetilde{D}_{i,n}} df$$

$$= k_{\mathrm{U}}\sqrt{E_{\mathrm{U}}} \mathbf{W}_i(-f'_{\mathrm{U}}) \mathbf{H}_i(f_{\mathrm{N}}) e^{-j2\pi f_{\mathrm{U}} D_i} \sum_{n=-\infty}^{\infty} a_{i,n}^{\mathrm{U}} e^{j\theta_{i,n}^{\mathrm{U}}} g(\widetilde{D}_{i,n}) e^{j2\pi f'_{\mathrm{U}} \widetilde{D}_{i,n}} \tag{63}$$

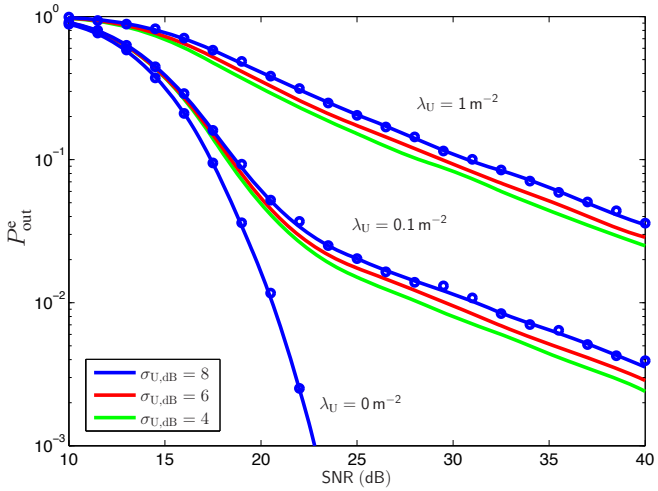

(a) $P_{\mathrm{out}}^{\mathrm{e}}$ versus the SNR of the NB link, for various spatial densities λ_{U} of the UWB interferers ($r_0 = 1\,\mathrm{m}$, $p^* = 10^{-2}$, $\mathsf{INR} = 50\,\mathrm{dB}$).

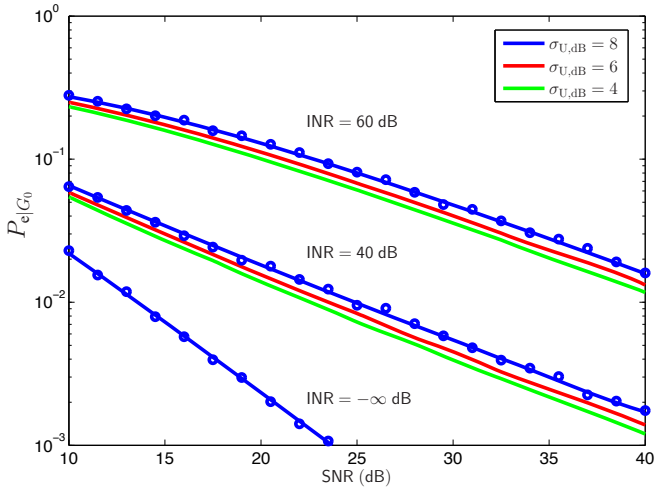

(b) $P_{\mathrm{e}|G_0}$ versus the SNR of the NB link, for various values of the INR ($r_0 = 1\,\mathrm{m}$, $G_0 = 0$, $\lambda_{\mathrm{U}} = 0.1\,\mathrm{m}^{-2}$).

Fig. 3. Error performance of a BPSK NB victim link subject to DS-BPAM UWB interferers (*solid lines*: semi-analytical results; *circles*: physical-level simulations).

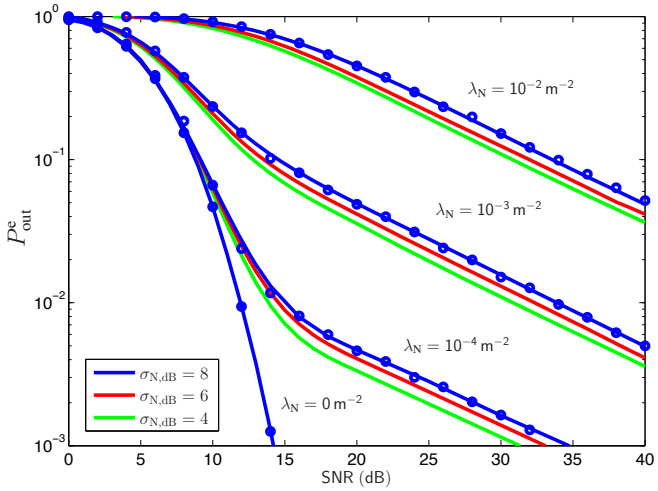

(a) $P_{\mathrm{out}}^{\mathrm{e}}$ versus the SNR of the UWB link, for various spatial densities λ_{N} of the NB interferers ($r_0 = 1\,\mathrm{m}$, $p^* = 10^{-2}$, $\mathsf{INR} = 50\,\mathrm{dB}$).

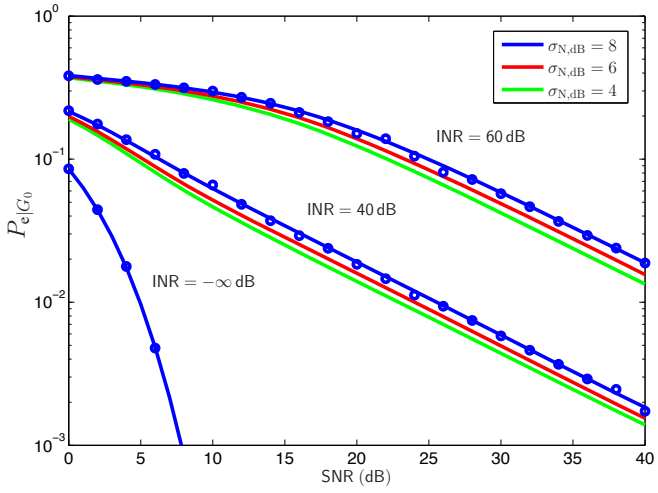

(b) $P_{\mathrm{e}|G_0}$ versus the SNR of the NB link, for various values of the INR ($r_0 = 1\,\mathrm{m}$, $G_0 = 0$, $\lambda_{\mathrm{N}} = 0.01\,\mathrm{m}^{-2}$).

Fig. 4. Error performance of a DS-BPAM UWB victim link subject to BPSK NB interferers (*solid lines*: semi-analytical results; *circles*: physical-level simulations).

at the frequency $f_{\mathrm{N}} = 5010\,\mathrm{MHz}$; a typical value of P_{N} is $20\,\mathrm{dBm}$ (e.g., for Bluetooth or WLAN systems). Therefore, in this scenario, Fig. 4(a) shows that for $\mathsf{INR} = 50\,\mathrm{dB}$, $\mathsf{SNR} = 20\,\mathrm{dB}$, and $\lambda_{\mathrm{N}} = 0.01\,\mathrm{m}^{-2}$, the UWB victim link experiences at least 40% outage. Similarly, Fig. 4(b) shows that with $\mathsf{INR} = 60\,\mathrm{dB}$, $\mathsf{SNR} = 20\,\mathrm{dB}$ and $\lambda_{\mathrm{N}} = 0.01\,\mathrm{m}^{-2}$, the UWB victim link experiences an average BEP greater than 10^{-1}. Therefore, despite the intrinsic robustness of UWB systems to NB interference, as known for SS systems, the aggregate NB interference on UWB systems represents an important issue that must be taken into account to ensure coexistence, and proper countermeasures must be employed. For example, [22] and [24] propose the adoption of proper spreading sequences to increase the allowable interference level. The figures also show that the error performance of the victim link is relatively insensitive to the shadowing parameters σ_{N} or σ_{U} characterizing the channel of the interferers.

VI. Conclusion

Using tools from stochastic geometry, we introduced a mathematical model for coexistence in heterogeneous wireless networks composed of both NB and UWB nodes. We considered realistic channel models, which account for the propagation effects specific to NB and UWB channels. We studied two dual configurations which are relevant in understanding coexistence: 1) a NB victim link subject to the aggregate UWB interference, and 2) a UWB victim link subject to the aggregate NB interference. In both cases, we showed that the aggregate interference at the output of the victim (NB or UWB) receiver, when conditioned on the position of interferers, is Gaussian with a variance that can be related to a *skewed stable* distribution. On the other hand, when averaged over the position of the interferers, the aggregate interference has a *symmetric stable* distribution. We then characterized the error performance in terms of outage and average error probabilities, and performed physical-level simulations to validate the analytical methodology proposed in this paper. The simulation results are in good agreement with the analytical results, indicating that the proposed methodology eliminates the need for time-consuming physical-level simulations in order to obtain the error performance.

We applied the proposed framework to uncover important issues regarding the coexistence between NB and UWB systems. While in many scenarios the impact of a *single* UWB interferer on a NB link is negligible due to PSD limits imposed on UWB transmission, this may not be the case when considering the *aggregate effect* of many UWB transmitting nodes. For example, we found that UWB node densities of $\lambda_{\mathrm{U}} = 0.1\,\mathrm{m}^{-2}$ can produce non-negligible degradation to NB links. Since unregulated UWB devices easily reach such density in suburban areas, the aggregate effect of the interferers must be considered in the system design to allow coexistence between heterogeneous devices. For the dual case of UWB systems affected by NB interference, we showed that a scenario with strong and dense NB interferers producing high aggregate interference is not unlikely. Thus, the inherent robustness of UWB systems to NB interference may not be sufficient to ensure an acceptable error performance when the NB node density is $\lambda_{\mathrm{N}} = 0.01\,\mathrm{m}^{-2}$. Therefore, additional countermeasures are necessary to increase the robustness of the UWB link.

Our work helps in understanding and assessing the *aggregate effect* of multiple interferers, subject to realistic channel models. Such effect is key in determining coexistence in heterogeneous networks, and suggests that spectral regulations that are based solely on the PSD of individual transmitters do not necessarily protect a victim receiver against interference.

Acknowledgments

The authors would like to thank G. J. Foschini, L. Greenstein, L. A. Shepp, and J. H. Winters for their helpful suggestions.

Appendix A
Derivation of $\mathbf{X}_i$ in (12)

To derive the expression for $\mathbf{X}_i$ in (12), we start from (11) and we use Parseval's relation to obtain (62) at the top of the previous page. Note that $\mathbf{W}_i(f)$ and $\mathbf{H}_i(f)$ correspond to UWB spectra, and therefore are approximately constant over the frequencies of the NB spectrum $\mathbf{G}(f - f_{\mathrm{N}})$. We can thus move the terms $\mathbf{W}_i(f \pm f_{\mathrm{U}})$ and $\mathbf{H}_i(f)$ outside of the integrals and obtain (63) at the top of the previous page. This is the result in (12) and the derivation is complete.

Appendix B
Derivation of the Distribution of A in (16)

Defining $\xi_i \triangleq e^{2\sigma_{\mathrm{U}} G_i}$, we use Campbell's theorem [32] to write the characteristic function of $A = \sum_{i=1}^{\infty} \frac{\xi_i}{R_i^{2\nu_{\mathrm{U}}}}$ for $\nu_{\mathrm{U}} > 1$ as

$$\phi_A(w) = \exp\left(-2\pi\lambda_{\mathrm{U}} \int_0^{\infty} \left[1 - \phi_{\xi}\left(\frac{w}{r^{2\nu_{\mathrm{U}}}}\right)\right] r dr\right),$$

where $\phi_{\xi}(w)$ is the characteristic function of ξ_i. Using the change of variable $|w| r^{-2\nu_{\mathrm{U}}} = t$, this can be rewritten as

$$\phi_A(w) = \exp\left(-\pi\lambda_{\mathrm{U}} |w|^{1/\nu_{\mathrm{U}}} \frac{1}{\nu_{\mathrm{U}}} \int_0^{\infty} \frac{1 - \mathbb{E}\left\{e^{j\,\mathrm{sign}(w)\xi_i t}\right\}}{t^{1/\nu_{\mathrm{U}}+1}} dt\right). \quad (64)$$

In [25, Appendix II] we showed that

$$\int_0^{\infty} \frac{1 - \mathbb{E}\left\{e^{j\,\mathrm{sign}(w)\xi_i t}\right\}}{t^{\alpha+1}} dt = \mathbb{E}\{\xi_i^{\alpha}\} \frac{C_{\alpha}^{-1}}{\alpha}\left[1 - j\,\mathrm{sign}(w)\tan\left(\frac{\pi\alpha}{2}\right)\right], \quad (65)$$

for $0 < \alpha < 1$, and C_{α} defined in (17). Using this relation, we rewrite (64) as

$$\phi_A(w) = \exp\left(-\gamma|w|^{\alpha}\left[1 - j\beta\,\mathrm{sign}(w)\tan\left(\frac{\pi\alpha}{2}\right)\right]\right), \quad (66)$$

where $\alpha = \frac{1}{\nu_{\mathrm{U}}}$, $\beta = 1$, and $\gamma = \pi\lambda_{\mathrm{U}} C_{1/\nu_{\mathrm{U}}}^{-1} \mathbb{E}\{\xi_i^{1/\nu_{\mathrm{U}}}\}$. Using the notation for stable distributions introduced in Footnote 14, we have

$$A \sim \mathcal{S}\left(\alpha = \frac{1}{\nu_{\mathrm{U}}},\ \beta = 1,\ \gamma = \pi\lambda_{\mathrm{U}} C_{1/\nu_{\mathrm{U}}}^{-1} e^{2\sigma_{\mathrm{U}}^2/\nu_{\mathrm{U}}^2}\right),$$

where we used the moment property of log-normal r.v.'s, i.e., $\mathbb{E}\{e^{kG}\} = e^{k^2/2}$ for $G \sim \mathcal{N}(0,1)$, in order to determine $\mathbb{E}\{\xi_i^{1/\nu_{\mathrm{U}}}\}$. This is the result in (16), and the derivation is complete.

APPENDIX C
DERIVATION OF THE DISTRIBUTION OF $\mathbf{Y}$ IN (18)

Defining $\mathbf{Q}_i \triangleq e^{\sigma_{\mathrm{U}} G_i}\mathbf{X}_i$, we use Campbell's theorem to write the characteristic function of $\mathbf{Y} = \sum_{i=1}^{\infty} \frac{\mathbf{Q}_i}{R_i^{\nu_{\mathrm{U}}}}$ for $\nu_{\mathrm{U}} > 1$ as

$$\phi_{\mathbf{Y}}(\mathbf{w}) = \exp\left(-2\pi\lambda_{\mathrm{U}} \int_0^{\infty} \left[1 - \phi_{\mathbf{Q}}\left(\frac{\mathbf{w}}{r^{\nu_{\mathrm{U}}}}\right)\right] r dr\right),$$

where $\phi_{\mathbf{Q}}(\mathbf{w})$ is the characteristic function of $\mathbf{Q}_i$. Note that $\mathbf{X}_i$, whose expression is given in (12), is CS due to the arguments presented in Section III-B2. As a result, the r.v. $\mathbf{Q}$ is also CS, i.e., $\phi_{\mathbf{Q}}(\mathbf{w}) = \phi_0(|\mathbf{w}|)$ for some $\phi_0(\cdot)$. As a result,

$$\phi_{\mathbf{Y}}(\mathbf{w}) = \exp\left(-2\pi\lambda_{\mathrm{U}} \int_0^{\infty} \left[1 - \phi_0\left(\left|\frac{\mathbf{w}}{r^{\nu_{\mathrm{U}}}}\right|\right)\right] r dr\right),$$

which, using the change of variable $|\mathbf{w}| r^{-\nu_{\mathrm{U}}} = t$, can be rewritten as

$$\phi_{\mathbf{Y}}(\mathbf{w}) = \exp\left(-\pi\lambda_{\mathrm{U}} |\mathbf{w}|^{2/\nu_{\mathrm{U}}} \frac{2}{\nu_{\mathrm{U}}} \int_0^{\infty} \frac{1 - \phi_0(t)}{t^{2/\nu_{\mathrm{U}}+1}} dt\right).$$

In [25, Appendix I] we showed that

$$\int_0^{\infty} \frac{1 - \phi_0(t)}{t^{\alpha+1}} dt = \frac{C_\alpha^{-1}}{\alpha} \mathbb{E}\{|\mathrm{Re}\{\mathbf{Q}_i\}|^{\alpha}\}, \tag{67}$$

with $0 < \alpha < 2$, and C_α defined in (17). We thus conclude that the characteristic function of $\mathbf{Y}$ has the simple form $\phi_{\mathbf{Y}}(\mathbf{w}) = \exp(-\gamma|\mathbf{w}|^{\alpha})$, with $\alpha = \frac{2}{\nu_{\mathrm{U}}}$, and $\gamma = \lambda_{\mathrm{U}} \pi C_{2/\nu_{\mathrm{U}}}^{-1} \mathbb{E}\{|\mathrm{Re}\{\mathbf{Q}_i\}|^{2/\nu_{\mathrm{U}}}\}$. Using the notation for stable distributions introduced in Footnote 15, we have

$$\mathbf{Y} \sim \mathcal{S}_{\mathrm{c}}\left(\alpha = \frac{2}{\nu_{\mathrm{U}}},\ \beta = 0,\right.$$
$$\left.\gamma = \pi\lambda_{\mathrm{U}} C_{2/\nu_{\mathrm{U}}}^{-1} e^{2\sigma_{\mathrm{U}}^2/\nu_{\mathrm{U}}^2} \mathbb{E}\{|\mathrm{Re}\{\mathbf{X}_i\}|^{2/\nu_{\mathrm{U}}}\}\right),$$

where we used again the moment property of log-normal r.v.'s. This is the result in (18), and the derivation is complete.

APPENDIX D
DERIVATION OF $\mathbf{X}_i$ IN (44)

The integral in (42) can be expressed as

$$\int_{-\infty}^{+\infty} \cos(2\pi f_{\mathrm{N}} t + \widetilde{\phi}_i) w(t) e^{-j2\pi f_{\mathrm{U}} t} dt = \frac{1}{2} \mathbf{W}(f_{\mathrm{U}} - f_{\mathrm{N}}) e^{j\widetilde{\phi}_i} \tag{68}$$

with $\widetilde{\phi}_i = \phi_i + 2\pi f_{\mathrm{N}} t_q$. We used the fact that $\mathbf{W}(f_{\mathrm{U}} + f_{\mathrm{N}}) = 0$, for carrier-based systems. Now, substituting (68) in (42), we can write

$$\mathbf{X}_i = k_{\mathrm{N}} \sqrt{P_{\mathrm{N}}} \alpha_i e^{j\phi_i} \mathbf{W}(f_{\mathrm{U}} - f_{\mathrm{N}}) \sum_{q=1}^{L} h_q e^{j2\pi f_{\mathrm{N}} t_q},$$

from which (44) is obtained.

REFERENCES

[1] M. Z. Win and R. A. Scholtz, "Impulse radio: How it works," *IEEE Commun. Lett.*, vol. 2, no. 2, pp. 36–38, Feb. 1998.

[2] ——, "Ultra-wide bandwidth time-hopping spread-spectrum impulse radio for wireless multiple-access communications," *IEEE Trans. Commun.*, vol. 48, no. 4, pp. 679–691, Apr. 2000.

[3] ——, "Characterization of ultra-wide bandwidth wireless indoor communications channel: A communication theoretic view," *IEEE J. Select. Areas Commun.*, vol. 20, no. 9, pp. 1613–1627, Dec. 2002.

[4] D. Cassioli, M. Z. Win, and A. F. Molisch, "The ultra-wide bandwidth indoor channel: from statistical model to simulations," *IEEE J. Select. Areas Commun.*, vol. 20, no. 6, pp. 1247–1257, Aug. 2002.

[5] A. F. Molisch, "Ultrawideband propagation channels-theory, measurements, and modeling," *IEEE Trans. Veh. Technol.*, vol. 54, no. 5, pp. 1528–1545, Sept. 2005.

[6] M. Z. Win, "Spectral density of random time-hopping spread-spectrum UWB signals," *IEEE Commun. Lett.*, vol. 6, no. 12, pp. 526–528, Dec. 2002.

[7] T. Q. S. Quek and M. Z. Win, "Analysis of UWB transmitted-reference communication systems in dense multipath channels," *IEEE J. Select. Areas Commun.*, vol. 23, no. 9, pp. 1863–1874, Sept. 2005.

[8] T. Q. S. Quek, M. Z. Win, and D. Dardari, "Unified analysis of UWB transmitted-reference schemes in the presence of narrowband interference," *IEEE Trans. Wireless Commun.*, vol. 6, no. 6, pp. 2126–2139, June 2007.

[9] W. Suwansantisuk, M. Z. Win, and L. A. Shepp, "On the performance of wide-bandwidth signal acquisition in dense multipath channels," *IEEE Trans. Veh. Technol.*, vol. 54, no. 5, pp. 1584–1594, Sept. 2005, special section on *Ultra-Wideband Wireless Communications–A New Horizon.*

[10] W. Suwansantisuk and M. Z. Win, "Multipath aided rapid acquisition: Optimal search strategies," *IEEE Trans. Inform. Theory*, vol. 53, no. 1, pp. 174–193, Jan. 2007.

[11] A. Swami, B. Sadler, and J. Turner, "On the coexistence of ultra-wideband and narrowband radio systems," in *Proc. Military Commun. Conf.*, vol. 1, McLean, VA, Oct. 2001, pp. 16–19.

[12] J. R. Foerster, "The performance of a direct sequence spread ultra-wideband system in the presence of multipath, narrowband interference and multi-user interference," in *Proc. of IEEE Conf. on Ultra Wideband Syst. and Technol. (UWBST)*, Baltimore, MD, May 2002, pp. 87–91.

[13] R. Fontana, "An insight into UWB interference from a shot noise perspective," in *Proc. of IEEE Conf. on Ultra Wideband Syst. and Technol. (UWBST)*, Baltimore, MD, May 2002, pp. 309–313.

[14] D. Dardari and G. Pasolini, "Simple and accurate models for error probability evaluation of IEEE802.11 DS-SS physical interface in the presence of Bluetooth interference," in *Proc. IEEE Global Telecomm. Conf.*, vol. 1, Taipei, TAIWAN, Nov. 2002, pp. 201–206.

[15] L. B. Milstein, S. Davidovici, and D. L. Schilling, "The effect of multiple-tone interfering signals on a direct sequence spread spectrum communication system," *IEEE Trans. Commun.*, vol. 30, no. 3, pp. 436–446, Mar. 1982.

[16] R.-H. Dou and L. B. Milstein, "Error probability bounds and approximations for DS spread-spectrum communication systems with mutiple tone or multiple access interference," *IEEE Trans. Commun.*, vol. 32, no. 5, pp. 493–502, May 1984.

[17] M. Moeneclaey, M. V. Bladel, and H. Sari, "Sensitivity of multiple-access techniques to narrow-band interference," *IEEE Trans. Commun.*, vol. 49, no. 3, pp. 497–505, Mar. 2001.

[18] L. Zhao and A. M. Haimovich, "Performance of ultra-wideband communications in the presence of interference," *IEEE J. Select. Areas Commun.*, vol. 20, no. 9, pp. 1684–1691, Dec. 2002.

[19] M. M. Hämäläinen, R. Tesi, and J. Iianatti, "On the UWB system performance studies in AWGN channel with interference in UMTS band," in *Proc. of IEEE Conf. on Ultra Wideband Syst. and Technol. (UWBST)*, Baltimore, MD, May 2002, pp. 321–325.

[20] M. M. Hämäläinen, R. Tesi, J. Iianatti, and V. Hovinen, "On the performance comparison of different UWB data modulation schemes in AWGN channel in the presence of jamming," in *Proc. IEEE Radio and Wireless Conf.*, (RAWCON), Boston, MA, Aug. 2002, pp. 83–86.

[21] M. M. Hämäläinen, V. Hovinen, R. Tesi, J. H. J. Iinatti, and M. Latva-aho, "On the UWB system coexistence with GSM900, UMTS/WCDMA, and GPS," *IEEE J. Select. Areas Commun.*, vol. 20, no. 9, pp. 1712–1721, Dec. 2002.

[22] A. Giorgetti, M. Chiani, and M. Z. Win, "The effect of narrowband interference on wideband wireless communication systems," *IEEE Trans. Commun.*, vol. 53, no. 12, pp. 2139–2149, Dec. 2005.

[23] N. C. Beaulieu and D. J. Young, "Designing time-hopping ultrawide bandwidth receivers for multiuser interference environments," *Proc. IEEE*, vol. 97, no. 2, pp. 255–284, Feb. 2009, special issue on *Ultra-Wide Bandwidth (UWB) Technology & Emerging Applications*.

[24] M. Chiani and A. Giorgetti, "Coexistence between UWB and narrowband wireless communication systems," *Proc. IEEE*, vol. 97, no. 2, pp. 231–254, Feb. 2009, special issue on *Ultra-Wide Bandwidth (UWB) Technology & Emerging Applications*.

TABLE III
NOTATION AND SYMBOLS.

Symbol	Usage
$\mathbb{E}\{\cdot\}$	Expectation operator
$\mathbb{P}\{\cdot\}$	Probability operator
$*$	Convolution operator
$\mathbb{V}\{\cdot\}$	Variance operator
$\mathrm{Re}\{\cdot\}$	Real part operator
$\mathcal{N}(\mu, \sigma^2)$	Gaussian distribution with mean μ and variance σ^2
$\mathcal{N}_{\mathrm{c}}(0, \sigma^2)$	CS complex Gaussian distribution, with i.i.d. $\mathcal{N}(0, \sigma^2/2)$ real and imaginary parts
$\mathcal{S}(\alpha, \beta, \gamma)$	Stable distribution with characteristic exponent α, skewness β, and dispersion γ
$\mathcal{S}_{\mathrm{c}}(\alpha, \beta, \gamma)$	CS complex stable distribution, with $\mathcal{S}(\alpha, \beta, \gamma)$ real and imaginary components
$\mathcal{U}(a, b)$	Uniform distribution in the interval $[a, b]$
$s_i^{\mathrm{N}}(t), s_i^{\mathrm{U}}(t)$	Transmitted NB and UWB signals associated with the ith interferer
$\widetilde{h}_i^{\mathrm{N}}(t), \widetilde{h}_i^{\mathrm{U}}(t)$	Overall NB and UWB channel impulse responses associated with the ith interferer
$\nu_{\mathrm{N}}, \nu_{\mathrm{U}}$	Amplitude loss exponents of NB and UWB channels
$\sigma_{\mathrm{N}}, \sigma_{\mathrm{U}}$	Shadowing coefficients of NB and UWB channels
$T_{\mathrm{N}}, T_{\mathrm{U}}$	Symbol periods of NB and UWB signals
$E_{\mathrm{N}}, E_{\mathrm{U}}$	Transmitted symbol energy of NB and UWB signals

[25] M. Z. Win, P. C. Pinto, and L. A. Shepp, "A mathematical theory of network interference and its applications," *Proc. IEEE*, vol. 97, no. 2, pp. 205–230, Feb. 2009, special issue on *Ultra-Wide Bandwidth (UWB) Technology & Emerging Applications*.

[26] E. Sousa, "Performance of a spread spectrum packet radio network link in a Poisson field of interferers," *IEEE Trans. Inform. Theory*, vol. 38, no. 6, pp. 1743–1754, 1992.

[27] J. Ilow and D. Hatzinakos, "Analytic alpha-stable noise modeling in a Poisson field of interferers or scatterers," *IEEE Trans. Signal Processing*, vol. 46, no. 6, pp. 1601–1611, 1998.

[28] P. C. Pinto and M. Z. Win, "Communication in a Poisson field of interferers - Part I: Interference distribution and error probability," *IEEE Trans. Wireless Commun.*, 2009, accepted pending revision.

[29] ——, "Communication in a Poisson field of interferers - Part II: Channel capacity and interference spectrum," *IEEE Trans. Wireless Commun.*, 2009, accepted pending revision.

[30] M. Z. Win, P. C. Pinto, A. Giorgetti, M. Chiani, and L. A. Shepp, "Error performance of ultrawideband systems in a Poisson field of narrowband interferers," in *Proc. IEEE Int. Symp. on Spread Spectrum Techniques & Applications*, Manaus, BRAZIL, Aug. 2006, pp. 410–416.

[31] M. Haenggi, J. G. Andrews, F. Baccelli, O. Dousse, and M. Franceschetti, "Stochastic Geometry and Random Graphs for the Analysis and Design of Wireless Networks," *IEEE J. Select. Areas Commun.*, Sep. 2009.

[32] J. Kingman, *Poisson Processes*. Oxford University Press, 1993.

[33] D. P. Bertsekas and J. N. Tsitsiklis, *Introduction to Probability*. Athena Scientific, 2002.

[34] A. F. Molisch, *Wireless Communications*, 1st ed. Piscataway, New Jersey, 08855-1331: IEEE Press, J. Wiley and Sons, 2005.

[35] A. Goldsmith, *Wireless Communications*. Cambridge University Press, 2005.

[36] G. L. Stuber, *Principles of Mobile Communication*, 2nd ed. Norwell, MA 02061: Kluwer Academic Publishers, 2001.

[37] A. Conti, M. Z. Win, and M. Chiani, "Invertible bounds for M-QAM in fading channels," *IEEE Trans. Wireless Commun.*, vol. 4, no. 5, pp. 1994–2000, Sept. 2005.

[38] ——, "On the inverse symbol error probability for diversity reception," *IEEE Trans. Commun.*, vol. 51, no. 5, pp. 753–756, May 2003.

[39] A. Conti, M. Z. Win, M. Chiani, and J. H. Winters, "Bit error outage for diversity reception in shadowing environment," *IEEE Commun. Lett.*, vol. 7, no. 1, pp. 15–17, Jan. 2003.

[40] A. Conti, M. Z. Win, and M. Chiani, "Slow adaptive M-QAM with diversity in fast fading and shadowing," *IEEE Trans. Commun.*, vol. 55, no. 5, pp. 895–905, May 2007.

[41] A. Conti, W. M. Gifford, M. Z. Win, and M. Chiani, "Optimized simple bounds for diversity systems," *IEEE Trans. Commun.*, vol. 57, 2009, to appear.

[42] M. Z. Win and J. H. Winters, "Virtual branch analysis of symbol error probability for hybrid selection/maximal-ratio combining in Rayleigh fading," *IEEE Trans. Commun.*, vol. 49, no. 11, pp. 1926–1934, Nov. 2001.

[43] M. K. Simon and M.-S. Alouini, *Digital Communication over Fading Channels*. Wiley-IEEE Press, 2004.

[44] J. W. Craig, "A new, simple and exact result for calculating the probability of error for two-dimensional signal constellations," in *Proc. Military Commun. Conf.*, Boston, MA, 1991, pp. 25.5.1–25.5.5.

[45] W. M. Gifford, M. Z. Win, and M. Chiani, "Diversity with practical channel estimation," *IEEE Trans. Wireless Commun.*, vol. 4, no. 4, pp. 1935–1947, July 2005.

[46] M. Z. Win, G. Chrisikos, and A. F. Molisch, "Wideband diversity in multipath channels with nonuniform power dispersion profiles," *IEEE Trans. Wireless Commun.*, vol. 5, no. 5, pp. 1014–1022, May 2006.

[47] T. M. Cover and J. A. Thomas, *Elements of Information Theory*, 2nd ed. Wiley-Interscience, 2006.

[48] W. Feller, *An Introduction to Probability Theory and Its Applications*. Wiley, 1971, vol. 2.

[49] V. M. Zolotarev, *One-Dimensional Stable Distributions*. American Mathematical Society, 1986.

[50] A. Giorgetti and M. Chiani, "Influence of fading on the Gaussian approximation for BPSK and QPSK with asynchronous cochannel interference," *IEEE Trans. Wireless Commun.*, vol. 4, no. 2, pp. 384–389, 2005.

[51] G. Samoradnitsky and M. Taqqu, *Stable Non-Gaussian Random Processes*. Chapman and Hall, 1994.

[52] J. M. Holtzman, "A simple, accurate method to calculate spread-spectrum multiple-accesserr or probabilities," *IEEE Trans. Commun.*, vol. 40, no. 3, pp. 461–464, Mar. 1992.

[53] ——, "On using perturbation analysis to do sensitivity analysis: derivatives versus differences," *IEEE Trans. Autom. Control*, vol. 37, no. 2, pp. 243–247, Feb. 1992.

[54] J. Chambers, C. Mallows, and B. Stuck, "A method for simulating stable random variables," *J. Amer. Statist. Assoc.*, vol. 71, pp. 340–344, 1976.

Pedro C. Pinto (S'04) received the Licenciatura degree with highest honors in Electrical and Computer Engineering from the University of Porto, Portugal, in 2003. He received the M.S. degree in Electrical Engineering and Computer Science from the Massachusetts Institute of Technology (MIT) in 2006. Since 2004, he has been with the MIT Laboratory for Information and Decision Systems (LIDS), where he is now a Ph.D. candidate. His main research interests are in wireless communications and signal processing. He was the recipient of the MIT Claude E. Shannon Fellowship in 2007, the Best Student Paper Award at the IEEE International Conference on Ultra-Wideband in 2006, and the Infineon Technologies Award in 2003.

Andrea Giorgetti (M'04) received the Dr. Ing. degree (*magna cum laude*) in Electronic Engineering and the Ph.D. degree in Electronic Engineering and Computer Science from the University of Bologna, Bologna, Italy, in 1999 and 2003, respectively.

Since 2003, he has been with the Istituto di Elettronica e di Ingegneria dell'Informazione e delle Telecomunicazioni (IEIIT-BO), research unit at Bologna of the National Research Council (CNR), Bologna, Italy. In 2005 he has been a Researcher of the National Research Council, and since 2006 he is Assistant Professor at the II Engineering Faculty, University of Bologna, where he joined the Department of Electronics, Computer Sciences and Systems (DEIS).

During the spring of 2006 he was Research Affiliate at the Laboratory for Information and Decision Systems (LIDS), Massachusetts Institute of Technology (MIT), Cambridge, USA, working on coexistence issues between ultra wideband (UWB) and narrowband wireless systems. His research interests include ultrawide bandwidth communication systems, wireless sensor networks, and multiple-antenna systems. He was Cochair of the Wireless Networking Symposium at the IEEE Int. Conf. on Communications (ICC 2008), Beijing, CHINA, May 2008 and Cochair of the MAC track of the IEEE Wireless Comm. & Networking Conf. (WCNC 2009), Budapest, Hungary, Apr. 2009.

Moe Z. Win (F'04) received both the Ph.D. in Electrical Engineering and M.S. in Applied Mathematics as a Presidential Fellow at the University of Southern California (USC) in 1998. He received an M.S. in Electrical Engineering from USC in 1989, and a B.S. (*magna cum laude*) in Electrical Engineering from Texas A&M University in 1987.

Dr. Win is an Associate Professor at the Massachusetts Institute of Technology (MIT). Prior to joining MIT, he was at AT&T Research Laboratories for five years and at the Jet Propulsion Laboratory for seven years. His research encompasses developing fundamental theory, designing algorithms, and conducting experimentation for a broad range of real-world problems. His current research topics include location-aware networks, time-varying channels, multiple antenna systems, ultra-wide bandwidth systems, optical transmission systems, and space communications systems.

Professor Win is an IEEE Distinguished Lecturer and elected Fellow of IEEE, cited for "contributions to wideband wireless transmission." He was honored with the IEEE Eric E. Sumner Award (2006), an IEEE Technical Field Award for "pioneering contributions to ultra-wide band communications science and technology." His papers have received several awards including the IEEE Communications Society's Guglielmo Marconi Best Paper Award (2008) and the IEEE Antennas and Propagation Society's Sergei A. Schelkunoff Transactions Prize Paper Award (2003). Other recognitions include the Laurea Honoris Causa from the University of Ferrara, Italy (2008), the Technical Recognition Award of the IEEE ComSoc Radio Communications Committee (2008), Wireless Educator of the Year Award (2007), the Fulbright Foundation Senior Scholar Lecturing and Research Fellowship (2004), the U.S. Presidential Early Career Award for Scientists and Engineers (2004), the AIAA Young Aerospace Engineer of the Year (2004), and the Office of Naval Research Young Investigator Award (2003).

Professor Win has been actively involved in organizing and chairing a number of international conferences. He served as the Technical Program Chair for the IEEE Wireless Communications and Networking Conference in 2009, the IEEE Conference on Ultra Wideband in 2006, the IEEE Communication Theory Symposia of ICC-2004 and Globecom-2000, and the IEEE Conference on Ultra Wideband Systems and Technologies in 2002; Technical Program Vice-Chair for the IEEE International Conference on Communications in 2002; and the Tutorial Chair for ICC-2009 and the IEEE Semiannual International Vehicular Technology Conference in Fall 2001. He was the chair (2004-2006) and secretary (2002-2004) for the Radio Communications Committee of the IEEE Communications Society. Dr. Win is currently an Editor for IEEE TRANSACTIONS ON WIRELESS COMMUNICATIONS. He served as Area Editor for *Modulation and Signal Design* (2003-2006), Editor for *Wideband Wireless and Diversity* (2003-2006), and Editor for *Equalization and Diversity* (1998-2003), all for the IEEE TRANSACTIONS ON COMMUNICATIONS. He was Guest-Editor for the PROCEEDINGS OF THE IEEE (Special Issue on UWB Technology & Emerging Applications) in 2009 and IEEE JOURNAL ON SELECTED AREAS IN COMMUNICATIONS (Special Issue on Ultra -Wideband Radio in Multiaccess Wireless Communications) in 2002.

Marco Chiani (SM'02) was born in Rimini, Italy, in April 1964. He received the Dr. Ing. degree (*magna cum laude*) in Electronic Engineering and the Ph.D. degree in Electronic and Computer Science from the University of Bologna in 1989 and 1993, respectively. Dr. Chiani is a Full Professor at the II Engineering Faculty, University of Bologna, Italy, where he is the Chair in Telecommunication. During the summer of 2001 he was a Visiting Scientist at AT&T Research Laboratories in Middletown, NJ. He is a frequent visitor at the Massachusetts Institute of Technology (MIT), where he presently holds a Research Affiliate appointment.

Dr. Chiani's research interests include wireless communication systems, MIMO systems, wireless multimedia, low density parity check codes (LDPCC) and UWB. He is leading the research unit of University of Bologna on cognitive radio and UWB (European project EUWB), on Joint Source and Channel Coding for wireless video (European projects Phoenix-FP6 and Optimix-FP7), and is a consultant to the European Space Agency (ESA-ESOC) for the design and evaluation of error correcting codes based on LDPCC for space CCSDS applications.

Dr. Chiani has chaired, organized sessions and served on the Technical Program Committees at several IEEE International Conferences. In January 2006 he received the ICNEWS award "For Fundamental Contributions to the Theory and Practice of Wireless Communications". He was the recipient of the 2008 IEEE ComSoc Radio Communications Committee Outstanding Service Award.

He is the past chair (2002-2004) of the Radio Communications Committee of the IEEE Communication Society and past Editor of Wireless Communication (2000-2007) for the IEEE TRANSACTIONS ON COMMUNICATIONS.